TAMPEREEN TEKNILLINEN YLIOPISTO
TAMPERE UNIVERSITY OF TECHNOLOGY

EETU SORSA

HYALURONAN HYDROGELS COMBINED WITH COLLAGEN I AIMED FOR CORNEAL REGENERATION

Master of Science thesis

Examiners:
Professor Minna Kellomäki
& Lic. Phil. Jennika Karvinen

Examiners and topic approved
by the academic board
27th March 2017

ABSTRACT

EETU SORSA: Hyaluronan Hydrogels Combined with Collagen I Aimed for Corneal Regeneration
Tampere University of Technology
Master of Science Thesis, 72 pages, 3 Appendix pages
May 2017
Master's Degree Programme in Materials Technology
Major: Polymers and Biomaterials
Examiners: Professor Minna Kellomäki & Lic. Phil. Jennika Karvinen

Keywords: hydrogel, hyaluronan, collagen, cornea, biomaterials, polymers, tissue engineering

Millions of people worldwide suffer from corneal blindness, with many of them facing the global shortage of high quality donor corneas. A variety of artificial corneas have been developed to combat this problem, and a few have already reached commercial level. Natural polymers have shown potential as materials for tissue-engineered corneas due to their good biocompatibility, availability and typically mild reaction conditions. The aim of this thesis was to develop and characterise two hyaluronan hydrogels with and without rat tail collagen I to be used as scaffolds for the regeneration of the corneal stroma.

The hyaluronan components were modified to achieve two different types of hydrazone crosslinking. The hydrazide components of type A gels were modified using adipic acid dihydrazide (ADH), and the ones of type B with carbodihydrazide (CDH), both with their corresponding aldehyde derivatives. The collagenous and non-collagenous hydrogels were distinguished using suffixes 1 and 2. The characterisation itself consisted of mechanical, viscoelastic and optical analyses, as well as stability, degradation and swelling measurements. Cell viability tests guiding the development were conducted by a collaborating research group alongside the material optimisation process.

The mechanical characteristics were expressed using second order elastic constants. The average values for gels A1 and A2 in respective order were (5.4 ± 1.1) kPa and (2.9 ± 1.1) kPa, and the ones for gels B1 and B2 were (6.7 ± 1.0) kPa and (7.3 ± 1.1) kPa. The addition of collagen produced somewhat conflicting results, since it improved the mechanical resilience of type B gels and weakened type A gels, indicating that collagen might have interfered with the crosslinking efficiency of the polymers. The CDH-modified type B gels showed improved stability and controlled swelling behaviour in the physiological environment. All the gels were transparent and with refractive indices between 1.33 and 1.34, which is slightly lower than the one of the corneal stroma (1.38). Type B gels had higher refractive indices than type A, presumably due to their higher crosslink density. Preliminary results from custom transmittance measurements showed slightly decreased transparency in the collagenous gels, as was expected. Collagen-content also decreased the swelling as well as the rate of enzymatic degradation in both gel types.

The results showed that the CDH-modified hyaluronan hydrogels were significantly more stable in the cell culture medium and had superior mechanical and optical properties compared to the ADH-modified gels. Based on the results, type B gels could have potential to be developed into hydrogels for corneal regeneration in the future. However, further examination would still be necessary on the collagen used in this study.

TIIVISTELMÄ

EETU SORSA: Kollageeni I:een yhdistetyt hyaluronaanihydrogeelit sarveiskalvovaurioiden korjaamiseen
Tampereen teknillinen yliopisto
Diplomityö, 72 sivua, 3 liitesivua
Toukokuu 2017
Materiaalitekniikan diplomi-insinöörin tutkinto-ohjelma
Pääaine: Polymeerit ja biomateriaalit
Tarkastajat: professori Minna Kellomäki & Lic. Phil. Jennika Karvinen

Avainsanat: hydrogeeli, hyaluronaani, kollageeni, sarveiskalvo, biomateriaalit, polymeerit, kudosteknologia

Maailmanlaajuisesti miljoonat ihmiset ovat sokeutuneet sarveiskalvovaurioiden seurauksena. Vakavimpia niistä hoidetaan yleisesti kuolleilta ihmisiltä saaduilla sarveiskalvosiirteillä, joiden puute kuitenkin vaikeuttaa potilaiden hoitoonpääsyä. Ongelman ratkaisemiseksi on kehitetty keinotekoisia sarveiskalvoja, joista osa on jo kaupallisessa käytössä. Perustuen luonnonpolymeerien hyvään kudosyhteensopivuuteen ja neutraaleihin valmistusolosuhteisiin tämän työn tavoitteena oli kehittää ja karakterisoida kaksi hyaluronaaniin perustuvaa hydrogeeliä sellaisenaan sekä rotan hännän kollageeniin yhdistettyinä.

Hyaluronaanikomponentteja muokattiin kemiallisesti kahden eri tyypin hydratsoniristisillan muodostamiseksi. Kumpikin geeli koostui aldehydi- ja hydratsidimodifioiduista komponenteista, jotka yhdessä muodostivat hydratsonisidoksen. Tyypin A geelien hyaluronihappoon liitettiin adipiinihapon dihydratsidiryhmä (ADH) ja vastaava aldehydiryhmä, kun taas tyypin B geelit modifioitiin karbodihydratsidiryhmällä (CDH) ja vastaavalla aldehydiryhmällä. Ei-kollageeniset ja kollageenia sisältävät geelit eroteltiin lisäksi numeroilla 1 ja 2 vastaavassa järjestyksessä. Geelien karakterisointi sisälsi mekaanisia, reologisia ja optisia mittauksia sekä stabiilisuus-, turpoamis- ja hajoamistestejä. Soluyhteensopivuustestit suoritti BioMediTechin Silmäryhmä Tampereella.

Geelien mekaanisia ominaisuuksia kuvattiin ns. toisen asteen elastisuusvakioilla, jotka geeleille A1 ja A2 olivat (5,4 ± 1,1) kPa ja (2,9 ± 1,1) kPa ja vastaavasti geeleille B1 ja B2 (6,7 ± 1,0) kPa ja (7,3 ± 1,1) kPa. Kollageenin lisäys tuotti ristiriitaisia tuloksia, sillä se vahvisti tyypin B geelejä, mutta heikensi tyypin A geelejä. Kollageenilla epäiltiin olevan vaikutusta geelien ristisilloittumiseen heikentämällä toisen geelityypin polymeerien ristisiltojen muodostumista. Tyypin B geelit olivat huomattavasti stabiilimpia fysiologisissa olosuhteissa. Kaikki geelit olivat läpinäkyviä ja niiden taitekertoimet välillä 1,33–1,34, mikä on hieman sarveiskalvon stroomaa (1,38) alhaisempi. Johtuen tiiviimmästä ristisilloittumisesta B-tyypin geelien taitekertoimet olivat suuremmat. Läpinäkyvyyttä tutkittiin modifioidulla transmittanssimittauksella, jonka perusteella todettiin kollageenin lisäyksen hieman heikentävän geelien läpinäkyvyyttä. Kollageeni myös hidasti geelien hajoamista ja alensi niiden turpoamisastetta.

Tulosten perusteella CDH-modifioidut, tyypin B geelit olivat huomattavasti kestävämpiä, vakaampia ja optisesti parempia kuin ADH-modifioidut tyypin A geelit. Johtopäätöksenä voidaan todeta, että tyypin B geelit voisivat olla varteenotettava vaihtoehto silmän sarveiskalvovaurioiden korjaamiseen. Työssä esiintyneiden laatuongelmien vuoksi kollageenin lisäämisen vaikutuksia tulisi kuitenkin tutkia vielä tarkemmin.

PREFACE

This Master of Science thesis was carried out for the Biomaterials and Tissue Engineering Group in Tampere University of Technology and for the Eye Group of BioMediTech Institute of Biosciences and Medical Technology in Tampere, Finland, as a part of the Human Spare Parts research programme.

I would like to express my gratitude to Professor Minna Kellomäki for giving me this opportunity to work and learn as a part of a professional research group, and to even expand the content of my thesis over its original scope. I would also like to thank professor Kellomäki for being my examiner and for giving expert advice during the thesis writing process, as well as for her inspiring university lectures in the field of tissue engineering.

I believe that during the past year I might have learned and developed myself more than during my whole university career before this, which is almost single-handedly thanks to my wonderful thesis advisor and examiner Lic. Phil. Jennika Karvinen. In her guidance, I have learned how to use a wide range of methods and equipment from the fields of materials science, chemistry, tissue engineering and even computer science, which I believe will be hugely beneficial for my future career.

I also want to thank Associate Professor Heli Skottman, Senior Researcher Tanja Ilmarinen and PhD student Laura Koivusalo from BioMediTech Eye Group for an extremely interesting topic, and for their professional guidance and collaboration along this research process.

Lastly, I would like to thank my friends and family for their encouraging (and sometimes pressuring) words, which gave me a gentle push forward at the times when I needed it.

Tampere, 22.5.2017

Eetu Sorsa

TABLE OF CONTENTS

LIST OF ABBREVIATIONS AND SYMBOLS

ADH	Adipic acid dihydrazide
AM	Amniotic membrane
ATR	Attenuated total reflection
CDH	Carbodihydrazide
CLP	Collagen-like peptide
DALK	Deep anterior lamellar keratoplasty
DMEM	Dulbecco's Modified Eagle Medium
DMSO	Dimethyl sulphoxide
ECM	Extracellular matrix
ESC	Epithelial stem cell
F-12	Ham's F-12 Nutrient Mixture
FACIT	Fibril Associated Collagens with Interrupted Triple helices
FTIR	Fourier transform infrared spectroscopy
GAG	Glycosaminoglycan
HA	Hyaluronic acid
HA-ADH	Adipic acid dihydrazide-modified hyaluronan
HA-CDH	Carbodihydrazide-modified hyaluronan
IOP	Intraocular pressure
IPN	Interpenetrating polymer network
KPro	Keratoprosthesis
LESC	Limbal epithelial stem cell
LSCD	Limbal stem cell deficiency
MW	Molecular weight
PBS	Phosphate-buffered saline
PDMS	Polydimethylsiloxane
PK	Penetrating keratoplasty
PTFE	Polytetrafluoroethylene
SPR	Surface Plasmon Resonance
SR	Swelling ratio
UV-vis	Ultraviolet-visible

1. INTRODUCTION

The cornea is the transparent ‘window’ into the eye, which contributes to a significant portion of its refractive power and provides protection to its delicate inner parts. As a tissue, the cornea is unique. To be able to produce a sharp image on the retina it possesses excellent refractive properties and, due to its avascularity, a metabolism that functions entirely through diffusion. The cornea is composed of a highly organised multilayer structure with five distinctive layers, which mainly consist of a variety of collagens and proteoglycans. (Freegard, 1997; Ruberti et al., 2011)

Since the cornea is the main immunological barrier between the external world and the eye, even minor ulcers may lead to serious infections, diseases or to a total loss of vision. Corneal diseases contribute to a remarkable part of blindness around the world, and their treatment often requires surgical intervention or even corneal substitution through allogenic transplantation (Whicher et al., 2001). The methods for corneal treatment are constantly improving, but there is a serious shortage of available donor corneas in all parts of the world, especially in developing countries where the prevalence of corneal diseases and traumas is higher and the possibility to receive appropriate medical care might not be available for all. This creates an increasing need for new solutions that are affordable, safe and independent of corneal donors, which in turn proposes a challenge to the tissue engineers trying to battle this problem.

With the progress in regenerative medicine, the development of tissue-engineered corneal substitutes has risen interest through the past decades, with applications ranging from natural materials and tissues to completely synthetic designs prepared from polymers created through recombinant DNA technology. Many research groups in the field have concentrated on the use of natural polymers and different composite structures that aim to mimic the natural corneal tissue. However, the aim of this thesis was not to produce a full-thickness implant, or to recreate the complicated layered structure of the cornea, but rather to prepare a prototype of a material that could be used in the future as a substrate for healing stromal damages. By combining the ECM-like properties of a hydrogel with collagen – a protein highly abundant in the natural cornea – this study aims to come one step closer to create a cell-friendly material for corneal regeneration.

For this thesis, two hyaluronan-based hydrogel materials were developed and combined with collagen I, which resulted in four different gel formulations. The aim was to create a material that meets the requirements set by the native corneal tissue, most importantly high biocompatibility, mechanical resilience and good optical properties. To evaluate gel performance in comparison to these requirements, an extensive array of material characterisation methods was utilised.

The first part of the thesis is theoretical, and it presents background information about the aims and requirements for the materials to be developed, and gives an insight into the current state and challenges of the research in the field today. The experimental part of the thesis consists essentially of different material characterisations, which include mechanical, optical, viscoelastic and stability tests, as well as chemical structure analyses and controlled enzymatic degradation experiments. The different methods are described and the results presented and discussed on the basis of the criteria presented in the theoretical part. Additionally, some points of interest regarding the current challenges in hydrogel characterisation methods will be discussed further in the discussion chapter.

The study was carried out for the Biomaterials and Tissue Engineering Group in Tampere University of Technology and for the Eye Group of BioMediTech, a joint institute of the University of Tampere and the Tampere University of Technology, concentrated on Biosciences and Medical Technology. The study was a part of the Human Spare Parts research program of BioMediTech.

THEORETICAL BACKGROUND

2. THE HUMAN CORNEA

Apart from being the protective barrier between the eye and the external environment, the cornea provides much of the eye's refractive power and helps the lens to produce a focused and sharp image on the retina. To make this possible, the cornea expresses some unique tissue features, such as high transparency, exceptional structural organisation, and the ability to maintain its immunological defence system without vascularisation (Freegard, 1997; Griffith et al., 2009).

From the viewpoint of materials science, the cornea could be classified as a composite structure with highly anisotropic and heterogeneous properties. More specifically, the cornea could be described as a fibre-reinforced hydrogel material that gets its bulk properties from the water-rich extracellular matrix (ECM) and its mechanical resilience from the lamellae of highly-organised collagen fibres. Even though as a tissue the cornea is relatively acellular, it has cellular layers that are essential to its transparency by upkeeping its metabolism and the optimal level of hydration (Freegard, 1997). The sizes of corneal structural components are well below the wavelength of visible light, which also contributes to its excellent optical clarity (Freegard, 1997).

The fact that the cornea is an avascular tissue brings up challenges for tissue engineers, whose aim is to mimic its features with scaffolds and implants. The task is not simple: creating a mechanically robust three-dimensional (3D) scaffold that enables a sufficient flow of nutrients and biomolecules to maintain the healthy corneal metabolism requires a very careful material design.

2.1 The multilayer structure of the cornea

The cornea is a transparent cellular structure consisting of five distinctive layers: three cellular layers with two membranes separating them. The layers of the cornea from anterior to posterior direction are epithelium, Bowman's layer, stroma, Descemet's membrane and endothelium. While the epithelium, the stroma and the endothelium are actual cell layers, Bowman's layer and Descemet's membrane are acellular basement membranes. The structure of the cornea is illustrated in Figure 2.1 below. (Freegard, 1997; Ruberti et al., 2011)

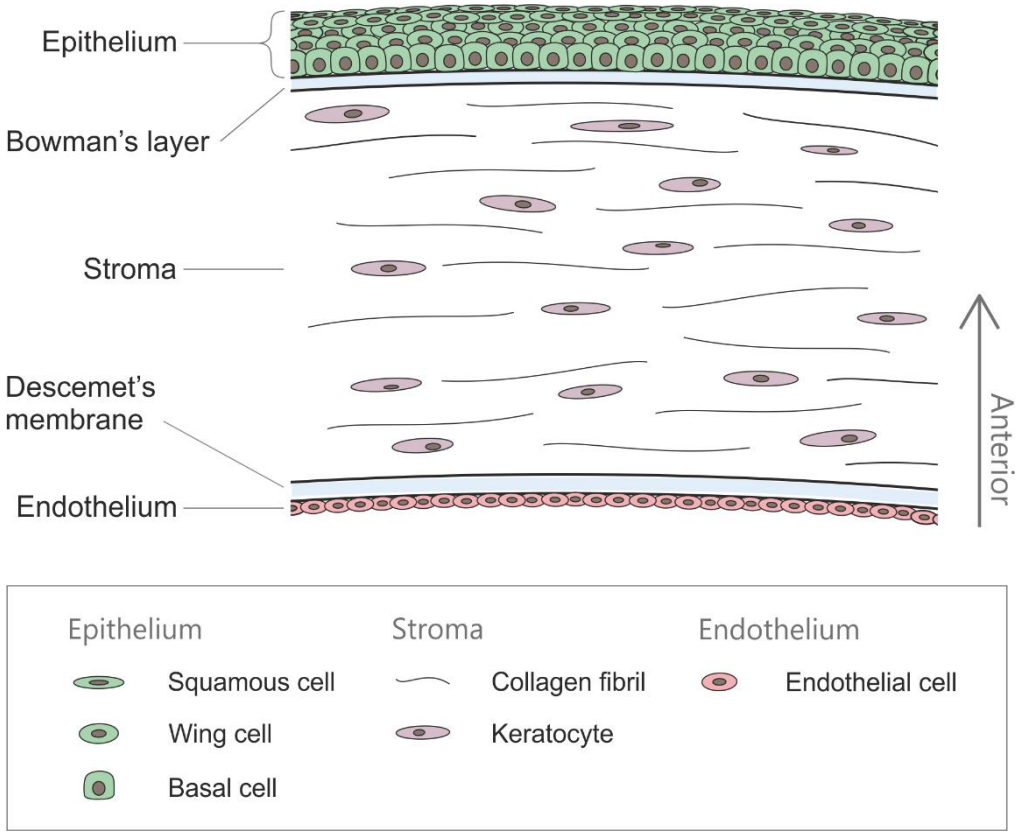

Figure 2.1. *A representative illustration of the structure and the cell types of the human cornea (modified from Ghezzi et al., 2015).*

Even though the cornea has five distinctive layers, most of its mechanical stiffness accounts for the two layers most abundant in collagen: the stroma and the Bowman's membrane (Dupps & Wilson, 2006). In their article, Dupps & Wilson (2006) note that the role of Bowman's membrane as a loadbearing structural component has been under discussion, referring to a study done by Seiler et al. in 1992. The latter states that the removal of Bowman's membrane does not actually cause any measurable changes in the mechanical properties of the cornea, which were determined through uniaxial stress-strain analysis of corneal samples with and without Bowman's layer (Seiler et al., 1992). Nevertheless, it can be concluded that the predominant component for corneal mechanical strength is the stroma. Apart from the actual tensile strength of the collagen fibres, some of the

most important factors contributing to its mechanical resilience are the orientation and branching between the different lamellae. The interlamellar branching provides increased resistance against shear forces, while the angular offsets of the lamellae add to cornea's ability to resist the intraocular pressure (IOP) (Dupps & Wilson, 2006).

The surface of the cornea has an aspherical geometry, which means that its anterior curvature does not form a part of a sphere. Instead, the corneal curvature is steeper in the central area than on the edges, and its thickness increases towards the sclera. (DelMonte & Kim, 2011) The average corneal diameter in adults is approximately 11.0 – 12.5 mm, with the central thickness being about 0,5 mm (Rüfer & Schröder, 2005, cited in Ghezzi et al., 2015).

Epithelium

Epithelium consists of 5 to 7 layers of cells attached to each other with tight junctions. The cells on the surface layer have plate-like morphology and are known as the squamous cells. The bottom layer of the epithelium consists of the basal cells, which are the cells that have most recently differentiated from their stem cells, known as limbal epithelial stem cells (LESC). (DelMonte & Kim, 2011) Between the layers of basal and squamous cells are the wing cells. The name comes from their morphology, since the cells are on their way to turn from round basal epithelial cells into flat squamous cells and express relatively irregular shapes (DelMonte & Kim, 2011). The limbal epithelial stem cells, or LESCs, are situated in the limbus, the border of the sclera and the cornea, from where they migrate towards the central cornea as they differentiate (Ahmad, 2012).

A healthy epithelium is essential for maintaining the transparency and good refractive properties of the cornea. Since the cornea does not have blood vessels, it doesn't have as efficient immunological defence ability as vascularised tissue. The cells on the surface are tightly packed together, which helps the epithelium to prevent pathogens from accessing the inner layers of the cornea. Additionally, the corneal epithelium is in constant process of self-renewal: as the squamous cells on the surface mature, they are shed into the environment with the tear fluid. The lost squamous cells are replaced by the underlying wing cells, which now become squamous cells. Therefore, the youngest cells are always the basal cells closest to Bowman's layer. This renewal is presumed to be another way of defending the eye from microbes and harmful substances. (Ruberti et al., 2011)

Stroma

The stroma is the thickest layer of the cornea and is composed of extracellular matrix rich in orientated collagen fibres, corneal keratocytes and proteoglycans (Michelacci, 2003). Reaching from Bowman's layer to Descemet's membrane, stroma spans about 80–90 % of the total corneal thickness (80–85 % according to DelMonte & Kim, 2011, 90 % according to Hassell & Birk, 2010). By weight, about 15 % of the stroma consists of collagen, while the rest is mainly water and biomolecules (Hassell & Birk, 2010). Of all stromal collagens, 75 % is of type I, which is why it was also used as one of the hydrogel

components in the experimental part of this thesis. In their article, Hassel & Birk state that apart from collagen I, the stroma has an unusually high amount of type VI collagen (17 % of stromal collagens) and smaller amounts of other types, like collagen VI and FACIT collagens. The transparency of the stroma is achieved through an exceptionally homogenous structure of collagen fibrils situated side-by-side in lamellae. These small, 25–30 nm thick fibrils are regularly spaced and have highly uniform diameter, which minimises light scattering and makes the stroma transparent. Additionally, the type of lamellar orientation is also believed to be optimal for the reduction of light scattering. (Ruberti et al., 2011)

Different types of corneal proteoglycans are located amongst the collagen fibrils, playing an important role in keeping the interfibrillar spaces even and in controlling the fibril diameters (Hassell & Birk, 2010). However, it has been noted (Komai & Ushiki, 1991, as cited in Ruberti et al, 2011) that the sizes of the lamellae are significantly different between the anterior and posterior parts of the stroma: The lamellae in the posterior are almost ten times wider and about two times thicker than the ones in the anterior part.

Descemet's membrane

Descemet's membrane is a thick basement membrane dividing the stroma and the endothelium. It provides support for the posterior surface of the cornea, and is produced by the endothelial cell layer (Pavelka & Roth, 2010). Although Descemet's membrane was once thought to have no distinguishable structure (Jakus, 1956), it has later proven to express many types of organisation characteristic only to this membrane, such as hexagonal lattices and ladder-like structures (Pavelka & Roth, 2010).

Descemet's membrane is rich in collagens IV and VIII, and is mainly composed of different kind of proteins, such as fibronectin and laminin, and of proteoglycans like heparan, dermatan and keratin sulphate. While collagen IV can also be found in many other basement membranes, the type VIII is relatively rare elsewhere in the body. However, in Descemet's membrane, collagen VIII has been found essential for maintaining the phenotype of the endothelial cells residing on its surface. (Ihanamäki et al., 2004; Pavelka & Roth, 2010)

Endothelium

The posterior layer of the cornea is the endothelium, which is formed by a monolayer of cells with hexagonal shapes. Endothelium is an approximately 4-µm-thick layer of flat and tightly adhered cells with the main purpose of maintaining the relatively dehydrated state of the stroma, which is fundamental for its optical clarity. This mechanism keeping the stromal water-content steady at 78 % is known as deturgescence, fuelled by the osmotic gradient created by the ion pumps of the endothelial cells. (Delmonte & Kim, 2011)

The endothelial cells do not proliferate, but the cell density of about 3500 cells/mm^2 at birth normally lasts throughout the lifetime of an individual, with approximately 0.6 %

decrease per year. Additionally, the remaining endothelial cells have the ability to stretch themselves over time to cover the space left by the dead cells. (Delmonte & Kim, 2011)

Corneal collagens

In the cornea, as in many tissues of the body, different collagens are the main structural elements maintaining its shape and mechanical strength. What makes the corneal collagen fibrils different from the ones in other tissues is their highly uniform diameter, spacing and arrangement in the stroma. This precise structure and complex orientation of the collagen molecules are the principal reasons for the excellent transparency and high optical performance of the cornea. (Ihanamäki et al., 2004)

Although a wide range of different collagens is present, collagen I is the predominant type of collagen in the corneal tissue. At least 22 separate collagen types have been identified in the human eye, with six of them being exclusively found only in the ocular tissues. The collagen types characteristic to the corneal tissue apart from collagen I are the types V, VI, XII, XIII, XIV and XXIV. (Ihanamäki et al., 2004)

2.2 Corneal defects and their causes

Cornea has an essential role for helping the lens to create a focused image on the retina, as well as functioning as the outermost barrier between the external world and the eye. A failure in its immunological defence ability can lead to severe complications and even to complete loss of vision. In their review article, Whitcher *et al.* (2001) describe corneal diseases and injuries as some the most common causes of blindness in the world; second only to cataract, which is responsible for about 45 % of all the blindness worldwide. Although corneal ulcers are generally caused by diseases or injuries, defects may also result from various genetic disorders or states of malnutrition, such as the lack of certain vitamins (Whitcher et al., 2001). The different origins of corneal defects will be presented briefly in the following paragraphs.

Diseases

Diseases account for most of corneal ulcers, including a large variety of bacterial, viral and fungal infections, physiological disorders and different syndromes. Because the cornea is an avascular tissue, it heals relatively slow and its immune defence capabilities are inferior to the vascularised tissues of the body, making the cornea particularly susceptible to microbial infections and scarring (Whitcher et al., 2001). Additionally, Whitcher *et al.* note that the commonness of corneal diseases depends greatly on the economical and general situation of the country, and on the socioeconomic status of the patient, since effective care and eye clinics are often unavailable for many people in poor countries. Referring to an extensive review done by Négrel & Thylefors in 1998, Whitcher *et al.* (2001) state that the high prevalence of corneal diseases in the developing countries has even been described as a silent epidemic with a scale much larger than previously thought. Nevertheless, in both the developing and the developed countries there is currently a great

need for new treatment methods that could substitute the use of corneal keratoplasty and lessen the need for corneal donors.

The world's leading infectious disease causing blindness is trachoma, which is particularly dangerous in developing countries where modern operating facilities and eye-banks are rare. Severe trachoma is normally treated with penetrating keratoplasty (PK), but with weak outcome due to major corneal vascularisation and ocular surface problems. According to Whicher *et al.*, the most cost-efficient way to fight blindness caused by corneal diseases would be the development of comprehensive prevention programmes, especially in the developing countries. (Whitcher et al., 2001)

Unfortunately, some diseases cannot be prevented. Genetic disorders are not as common as infectious corneal diseases, but can cause conditions that are very complicated to treat. Instead of destroying the corneal tissue directly, genetic diseases often cause failure in the systems that are essential to maintain a healthy cornea. The treatment of genetic corneal diseases is a field that many research groups are focused on, involving advanced approaches in stem cell technologies and novel tissue engineering applications. An example of a serious corneal disorder that can originate both from injuries and hereditary diseases is the limbal stem cell deficiency (LSCD). LSCD is a term for severe corneal diseases that result from failure of the LESCs located at the border of the cornea and the sclera, which are responsible for maintaining the barrier between the transparent cornea and the vascular conjunctiva, and the renewal of the epithelium (Ahmad, 2012). If the LESCs stop regenerating, the conjunctival blood vessels invade the cornea and make it opaque, resulting in the loss of vision. Delivery of regenerated stem cells into the cornea inside or on the surface of a hydrogel, alike the ones presented in this thesis, could be one of the possible treatments for the LSCD in the future.

Injuries

The most common corneal injuries are scratches, cuts, chemical burns and contact lens problems. Statistically corneal injuries are not as common cause of blindness as diseases, because most of them are minor enough to be treated and healed through surgery or other means. Also, injuries often cause only monocular loss of vision rather than complete blindness, which means that the patients are not considered blind but only visually disabled (Négrel & Thylefors, 1998). However, even a minor corneal ulcer provokes a significant risk of infection, which may further on lead to a corneal disease and blindness. The occurrence of corneal injuries is especially high in areas with unrest and war in their recent history, where undetonated land mines and other weapons still cause injuries to civilians. Additionally, in developing countries corneal traumas caused by poor working conditions are especially high, which is why the most efficient approach in avoiding corneal blindness would be through different prevention programmes. (Whitcher et al., 2001; Négrel & Thylefors, 1998)

3. HYDROGELS FOR CORNEAL REGENERATION

Hydrogels are three-dimensional polymer networks with the capability of absorbing large amounts of water into their structure. Properties that mainly characterise a hydrogel and its swelling behaviour are the type and density of the crosslinks between its polymer chains. Based on this, hydrogels are generally classified into two groups: chemically crosslinked, ‘permanent’, and physically crosslinked, ‘reversible’, hydrogels (Hennink & Nostrum, 2002). Covalently bonded chemical crosslinks are typically stronger than physical crosslinks, which normally result from entanglements between the polymer chains, hydrogen bonds or other weak interactions between the molecules (Hennink & Nostrum, 2002). Apart from the type of bonding, crosslink density has a great effect on hydrogel stability and swelling. In this thesis, the focus is on chemical hydrogels utilizing so-called pseudo-click reactions between differently modified hyaluronan components.

Some of the most interesting features of hydrogel materials are their cell-friendly properties and similarity to the living tissue. Through incorporation of living cells into a hydrogel, researchers aspire to create fully degradable scaffolds that eventually would be replaced with healthy tissue generated by the cells inside. The 3D structure of hydrogels allows the cells to arrange into an architecture resembling the native ECM, which has been found to promote tissue growth (Kontturi, 2014). Because of their high water-content, hydrogels are also expected to allow effective transport of nutrients and other metabolic products of the cells, resembling the natural metabolism of the cornea, which functions entirely through diffusion. Hydrogels can also be modified and prepared under mild conditions and without the use of strong solvents that might limit cell viability, which further improves their suitability for biomedical applications. Unlike many other scaffold materials, hydrogels can often be delivered to the target site in minimally invasive ways, such as via injections. (Tan & Marra, 2010)

When developing a hydrogel imitating the properties of the human cornea, the material requirements can be roughly categorised based on the basic requirements for an implant, such as biocompatibility, and for the special features needed from the ocular tissue. The main requirements for a corneal implant are presented in Figure 3.1 below.

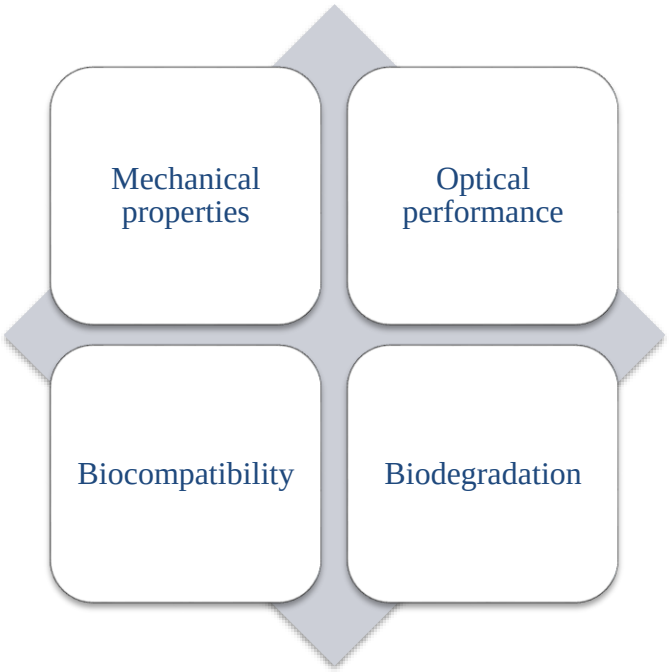

Figure 3.1. *The most relevant material requirements to be considered for a hydrogel aimed for corneal applications.*

Mechanically the cornea is very much like a hydrogel material. As described in Chapter 2.1, the cornea can be generally thought as a composite material consisting mainly of collagens, ECM and cells. Following this logic, the optimal material for this type of application would be a cell-friendly hydrogel matrix incorporated with collagen and ECM-producing cells. As new tissue is formed, the material should also degrade without releasing any undesirable by-products into the body. The purpose of the cornea is to provide refractive power for the eye, for which it expresses high transparency and good optical properties. Therefore, sufficient optical performance was also set as one of the material requirements. The importance of this requirement, however, was questioned afterwards (see Chapter 9.3) when evaluating the relationship between implant degradation and eyesight recovery times.

3.1 Hyaluronan-based hydrogels

Hyaluronan is a natural polysaccharide present everywhere in the body. It has a major role in organising and regulating the structure of the ECM, and controlling cell behaviour, such as their adhesion and morphology (Ossipov et al., 2010). It should be clarified that the term hyaluronan refers to all the physiological forms of the hyaluronic acid (HA), most commonly its sodium salt, while the term hyaluronic acid only refers to the actual HA compound. In this thesis, the term hyaluronan is primarily used, even when referring to the HA molecule itself.

3.1.1 Hyaluronan

Hyaluronan has been used in clinical practice already for over 30 years, and is still being studied for a huge variety of tissue engineering applications (Burdick & Prestwich, 2011). What makes it even more interesting from the viewpoint of product development, HA is a readily available and low-cost biomaterial. However, in its natural form, the half-life of hyaluronan in the body is only a few days at maximum before it is degraded by hyaluronidase enzymes (Burdick & Prestwich, 2011). Therefore, in the development of medical products it is often necessary to improve its persistence and shelf-life by increasing its molecular weight or cross-linking ratio and density.

The molecular structure of hyaluronan is highly conserved between mammalian species, consisting of two non-sulphated monosaccharide units: The D-glucuronic acid and the N-acetyl-D-glucosamine (Bulpitt et al., 1999; Price et al., 2007). These building blocks can polymerise into exceptionally large macromolecules with molecular weights reaching over millions of grams per mole (Price et al., 2007). On its own, hyaluronan is water-soluble and forms a gel when in contact with water. The viscoelastic behaviour of a HA-water solution is shear-thinning, which is why HA has a role as a lubricant in cartilage tissue in the joints (Price et al., 2007). As a crosslinked network, it withstands the hydrolytic degradation caused by water, and swells instead, forming a hydrogel. The strength and swelling capability of this kind of a gel is mainly determined by the strength and density of its crosslinks. The chemical structure of the repeating disaccharide unit of hyaluronan is presented in Figure 3.2 below.

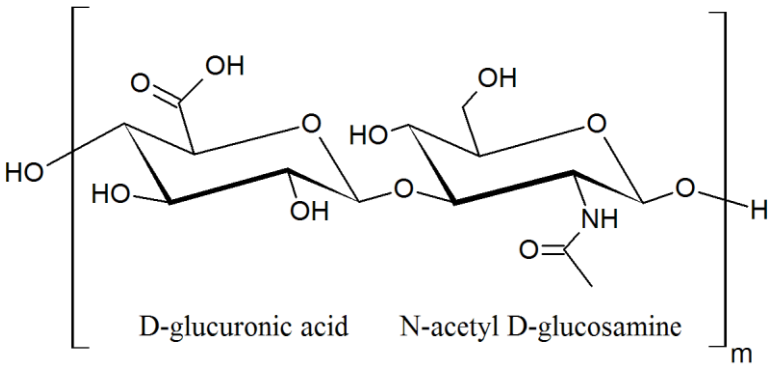

Figure 3.2. *The chemical structure of the repeating hyaluronan disaccharide complex.*

The fact that hyaluronan is a biomolecule native to the human body makes it a specially promising material for tissue engineering, with applications ranging from neural tissue regeneration (Seidlits, 2010) to skin fillers (Gold, 2007), and extensive research ongoing for corneal applications (Burdick & Prestwich, 2011). Additionally, it can be chemically modified to obtain tailorable properties for different applications, for example through

chemical conjugation of pharmaceuticals or preparation of HA-based nanocarriers. In addition, chemical crosslinking provides the means for controlling the mechanical properties and degradation rates of hyaluronan hydrogels. (Bulpitt et al., 1999; Ossipov et al., 2010) Some examples of hyaluronan modifications are acrylation, esterification and different crosslinking methods. However, many of these strategies produce materials that are not suitable to be crosslinked in the physiological environment, or involve strong crosslinking agents that make them unfavourable to be used in the physiological environment. (Bulpitt et al., 1999)

3.1.2 Modification and hydrazone-crosslinking of hyaluronan with functional aldehyde and hydrazide groups

Some methods of hyaluronan modification completely lack the use of external crosslinkers. An interesting approach is to modify two hyaluronan components with different functional groups capable of forming covalent crosslinks in the absence of additional crosslinking agents. This type of catalyst-free crosslinking resembles ‘click chemistry’, a class of chemical reactions that was first time introduced by the group of Dr. Barry Sharpless at the annual meeting of American Chemical Society in 1999 (Hein et al., 2008). Since then, click chemistry has become increasingly popular and is used in many kinds of chemical applications. It can be used for example to conjugate bioactive molecules into a polymer backbone, or to efficiently crosslink polymer chains together. The basis of click chemistry is in powerful reactions that involve simple reaction conditions, give high yields and do not require strong solvents. By definition, click chemistry products must also be easily purified and isolated, and stable under physiological conditions. (Kolb et al., 2001; Hein et al., 2008; Bulpitt et al., 1999.)

To achieve this catalyst-free covalent crosslinking, a chemical reaction known as the hydrazone bond was utilized. A hydrazone bond is formed through a relatively simple coupling reaction between aldehyde and hydrazide groups, and is typically characterised by its high yield, reversibility and excellent adaptability without requiring any harsh reaction conditions to occur (Jiang et al., 2014).

The HA polymers were modified with functional hydrazide and aldehyde groups based on the methods presented by Oommen *et al.* (2013), Bulpitt *et al.* (1999) Martínez et al. (2011) and Jia et al. (2006). However, similar protocols have been described in other reports as well. Apart from modifying the components with these functional groups, two different types of both HA components were prepared utilizing two different methods of aldehyde and hydrazide modification. The HA derivatives with an ADH-modified hydrazide components (HA-ALD1 & HA-ADH) were prepared per the procedures of Jia *et al.* (2006) and Bulpitt *et al.* (1999), and the HA components with a CDH-modified hydrazide component (HA-ALD2 & HA-CDH) were prepared following the protocols of Martínez *et al.* (2011) and Oommen *et al*. (2013).

The hydrogel tests initially started solely with the gels involving the ADH-modification (later referred to as the type A), but were extended to the CDH-modified gels (type B) due to the insufficient stability of the type A gels. Apart from being more stable when immersed in the cell culture medium, type B gels also proved mechanically and optically better to the type A. The superior hydrolytic stability of the CDH-linkage owed to the adjacent nitrogen atom N^3 providing resonance stabilisation to the CDH-bond. Oommen *et al.* describe (2013) this stabilisation analogous to the phenomenon known in chemistry as the 'alpha effect'. (Oommen et al., 2013)

Syntheses of the aldehyde-modified hyaluronan derivatives HA-ALD1 and HA-ALD2

The aldehyde-modified component in type A gels, HA-ALD1, was produced by reacting HA with an equivalent molar amount of sodium periodate ($NaIO_4$). This caused the oxidation of the vicinal hydroxyl groups on the C2–C3 carbons of the glucuronic acid moiety of the HA complex, resulting in two aldehyde groups. The steps of the HA-ALD1 and HA-ALD2 modifications are illustrated in Figure 3.3 and Figure 3.4 below in respective order.

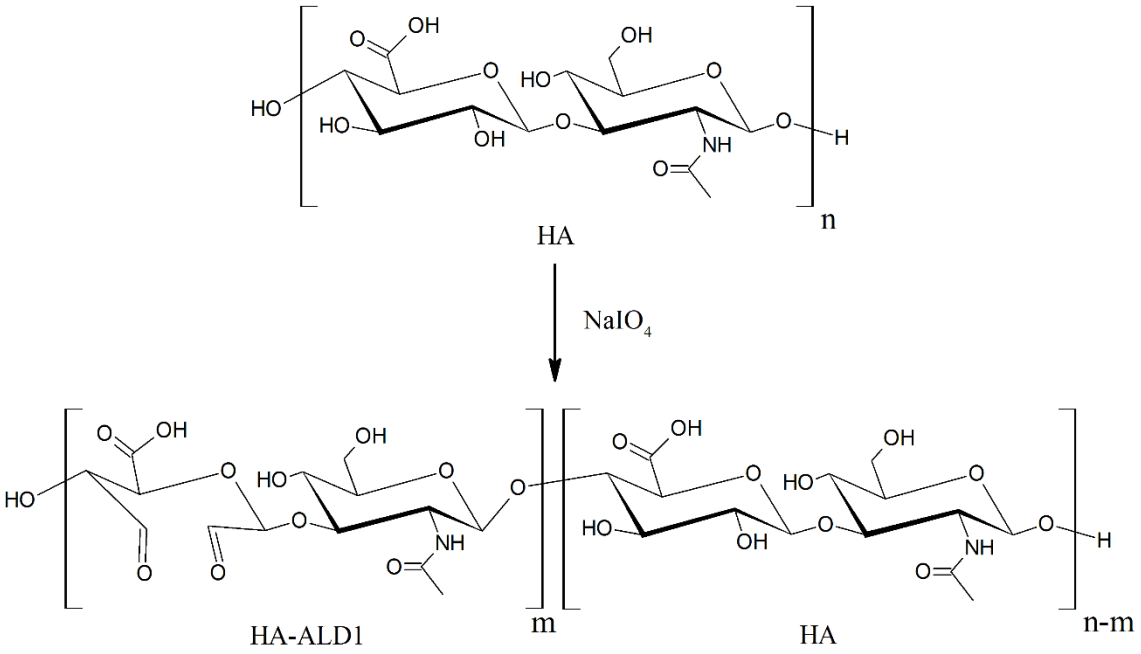

Figure 3.3. *Synthesis of the aldehyde-modified hyaluronan component HA-ALD1.*

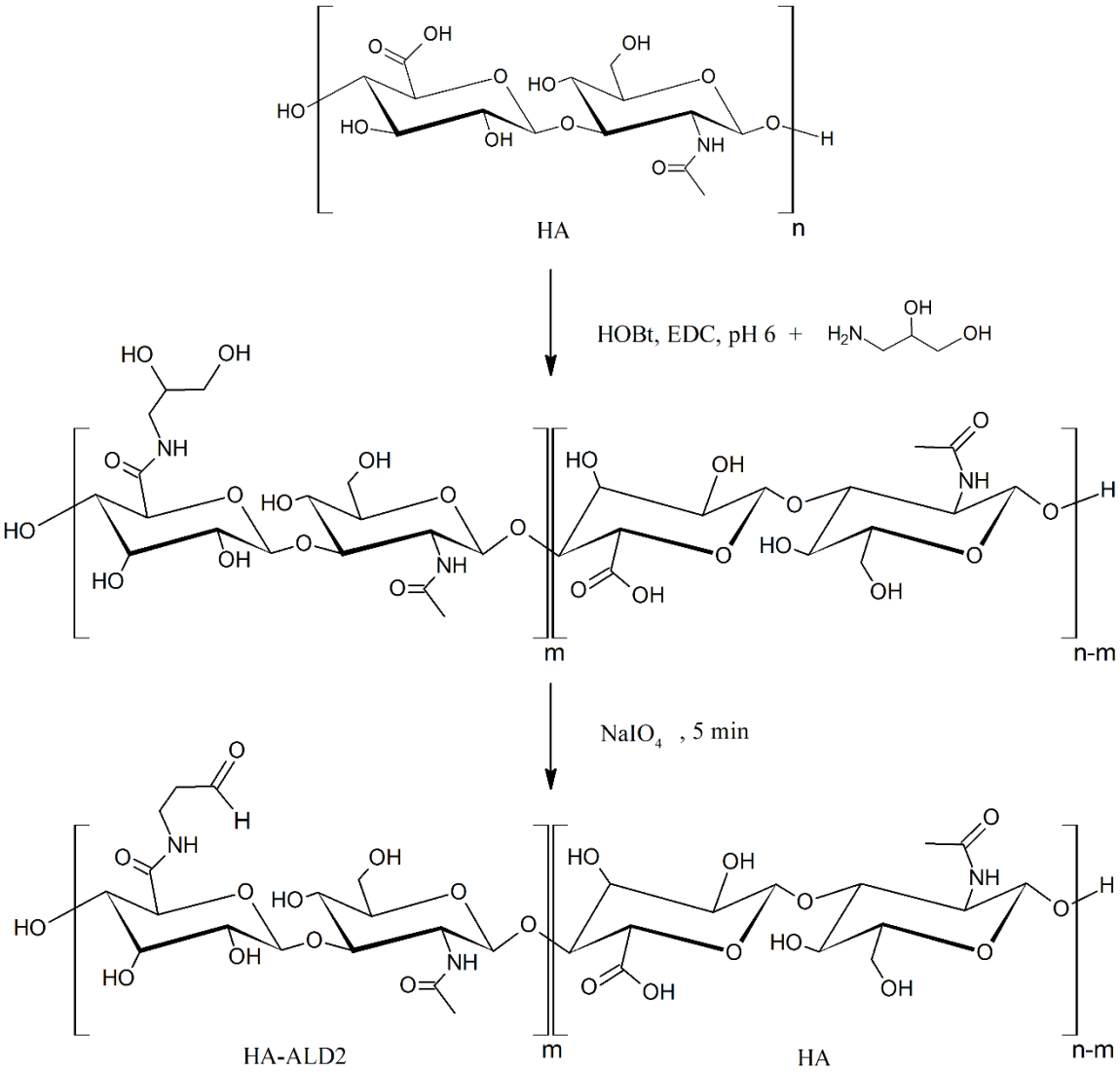

Figure 3.4. *Synthesis of the aldehyde-modified hyaluronan component HA-ALD2.*

The gel type B aldehyde component, HA-ALD2, was modified through selective oxidation of diol-modified HA. The main difference between the two modifications is that in the HA-ALD2 derivative the hyaluronan sugar ring structure was preserved, while the HA-ALD1 modification broke it to form the dialdehyde groups. Preserved ring structure provided the HA-ALD2 component with improved stability.

Syntheses of the hydrazide-modified hyaluronan derivatives HA-ADH and HA-CDH

The syntheses of the ADH and CDH-modified hyaluronan components, HA-ADH and HA-CDH, were both done by reacting the carboxylic groups of the HA molecule with an excess of either ADH or CDH in the presence of 1-hydroxybentzotriazole (HOBt) and 1-Ethyl-3-[3-(dimethylamino)propyl]-carbodiimide (EDC). The ADH reagent creates a 10-atom crosslink between the two hyaluronan polymers due to its internal aliphatic chain, while the CDH provides only a 5-atom bridge between the polymers. However, not hav-

ing the aliphatic carbon chain gives the CDH-modified hyaluronan improved water solubility compared to the ADH-modified component (Oommen et al., 2013). The chemical basis of the two hydrazide modifications are presented in Figures 3.5 and 3.6.

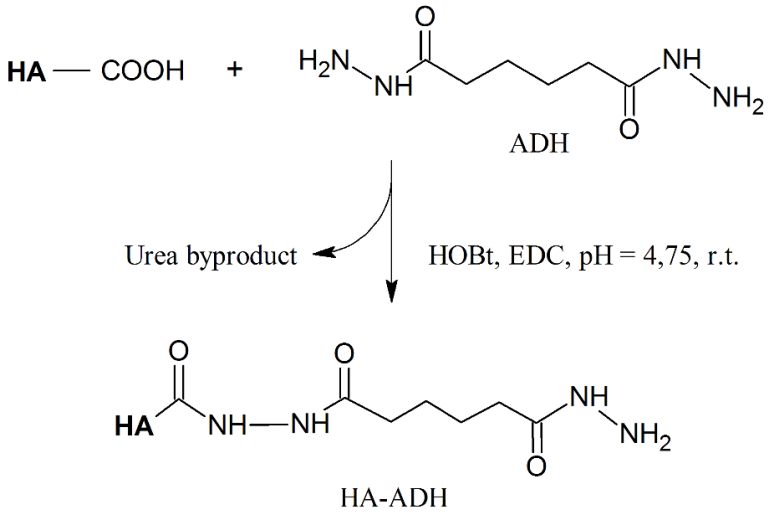

Figure 3.5. *Synthesis of the ADH-modified hyaluronan component.*

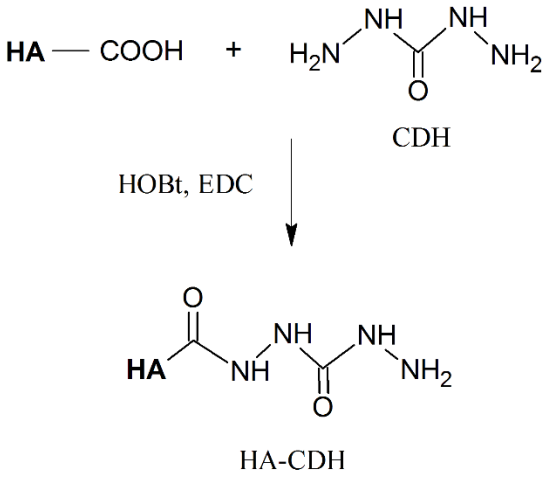

Figure 3.6. *Synthesis of the CDH-modified hyaluronan component.*

Hydrazone crosslinking of the modified hyaluronan components

Upon mixing, the hydrazone bond is spontaneously formed between the aldehyde and hydrazide hyaluronan derivatives. This way two different gels, HA-ALD1 + HA-ADH and HA-ALD2 + HA-CDH, were formed. The representative chemical structures of both hydrogels are presented in the following Figures 3.7 and 3.8.

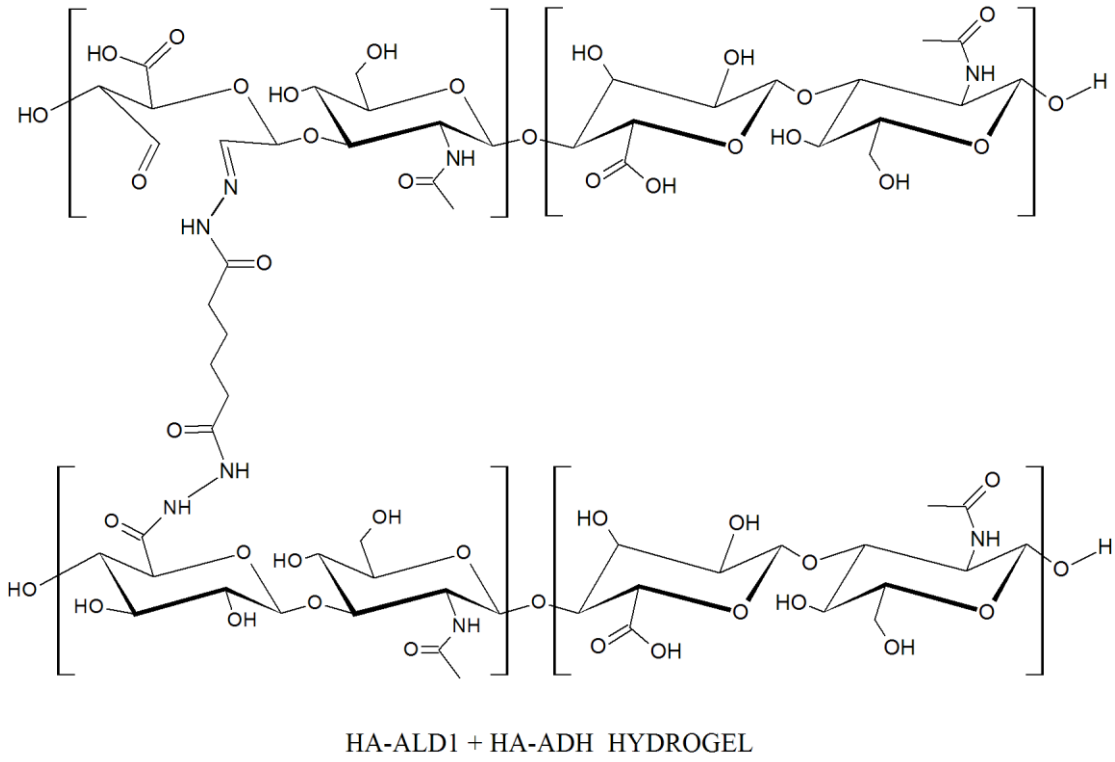

Figure 3.7. *Representative chemical structure of the hydrazone-crosslinked type A hydrogel from the HA-ALD1 and HA-ADH hyaluronan derivatives.*

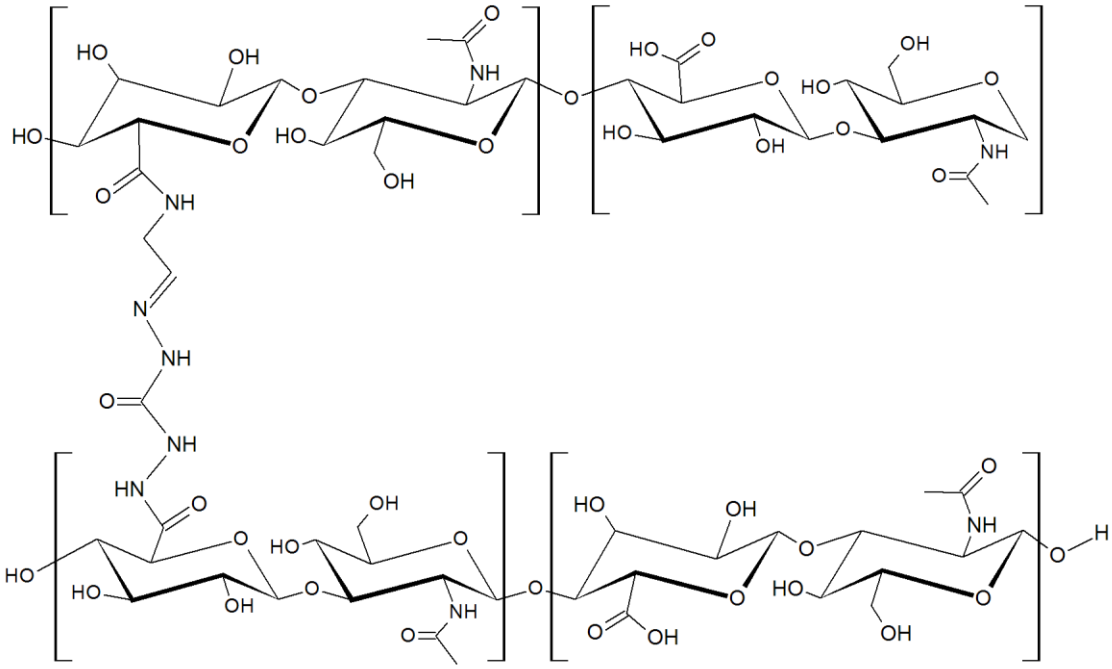

Figure 3.8. *Representative chemical structure of the hydrazone-crosslinked type B hydrogel from the HA-ALD2 and HA-CDH hyaluronan derivatives.*

As can be seen from the hydrogel chemical structures, the most important differences are in the preserved ring-structure of the type B gel, and the longer molecular bridge between the hyaluronan polymers in the gel type A.

3.2 Collagen-based hydrogels

As presented in Chapter 2, the cornea has been described (Griffith et al., 2009) as a hydrogel material that composes mainly of collagen, cells and proteoglycans. Apart from functioning as a reinforcing component in a hydrogel matrix, its low immunogenicity and ability to promote tissue growth have made collagen a special subject of interest for tissue engineers, especially in ophthalmology. It has been studied for numerous corneal applications, including different co-polymeric scaffolds incorporated with collagen and ECM components to promote the production of collagen, as well as corneal implants composed primarily from collagen. (Wang & Spector, 2009; Xiao et al., 2013) In this chapter, an overview and a few examples of collagen-based hydrogels in regenerative medicine will be briefly presented.

Collagen hydrogels

Collagen is abundantly available and has good properties to be used in a tissue-engineered corneal scaffold. Collagen spontaneously forms a gel when water is added, which makes it a relatively easy material to manufacture. It can work as a scaffold to culture corneal cells, such as stromal fibroblasts, which can proliferate and secrete new ECM material. (Borene et al., 2004; Shah et al., 2008) However, for corneal applications, collagen gels often require further processing to strengthen them, for example through compression (Xiao et al., 2014) and addition of crosslinking agents, which are often required to prevent rapid degradation of collagen in the physiological environment (Shah et al., 2008).

The problems with collagens from natural sources have been the inconsistencies in their quality and the adverse immunological reactions they might cause in the recipient (Lynn et al., 2004). Recombinant technology could resolve these problems, but is still an expensive method to use in large scale. In research, however, recombinant collagens in corneal applications have already shown promising results on both pre-clinical and clinical stages. Griffith *et al.* (2008) successfully manufactured hydrogel corneal substitutes from recombinant human collagens (RHC) I and III, which expressed similar properties to the native cornea. They showed high transparency, functional diffusion of nutrients and sufficient mechanical strength for implantation. During a 12-month *in vivo* study in pig models, these hydrogels supported the generation of nerves and tissue, and the proliferation of corneal cells. Although both collagen types possessed very similar properties, Griffith *et al.* reported that the RHC III implant showed superior strength and optical properties compared to the one of RHC I. (Griffith et al., 2008)

Clinical tests have also been conducted for corneal substitutes made of RHC III. In continuance to the research of Griffith *et al.* (2008), Fagerholm *et al.* (2009) implanted the same materials in 10 human subjects, showing promising results after a 6–7-month follow-up period. The operated eyes did not encounter adverse reactions, such as rejection or inflammation, and developed an even host-graft interface and smooth surface without distinguishable difference to the unoperated corneas. At the time of examination, the operated eyes showed good tissue integration and normal ocular pressure, with constantly improving visual acuity and surface quality. Fagerholm *et al.* (2009) concluded the results to be highly encouraging, but note that more comprehensive and longer-term clinical tests would still be needed to properly evaluate the clinical potential of these biomimetic corneal substitutes.

Collagen-incorporated hydrogels

There are numerous publications regarding collagen-based composite hydrogels targeted for ophthalmological applications. Many of them are copolymers that aim to compositionally resemble the structure of the corneal stroma, and some consist of a collagen matrix incorporated with cells and corneal ECM components (Borene et al., 2004; Myung et al., 2008).

In 2004, Borene *et al.* (2004) manufactured a prototype of a collagen-based stromal substitute incorporated with stromal fibroblasts, which showed features of natural wound healing response. The fibroblasts could migrate freely within the matrix and produced typical ECM molecules such as proteoglycans and collagen. In a study by Chen *et al.* (2005), a scaffold with a combination of collagen, chitosan and sodium hyaluronate was prepared and its biocompatibility was studied using rabbit corneal cells. With an optimal component ratio of 20 % collagen, 10 % chitosan and 0,5 % sodium hyaluronate the material showed good cell response and optical clarity (Chen et al., 2005).

Based on many publications, collagenous hydrogels have shown promising results and the use of different collagens has maintained its popularity among the development of biomimetic corneal substitutes. Through different processing and crosslinking strategies, the mechanical strength and biocompatibility of collagen-based scaffolds have been improved over the time. Furthermore, the advances in recombinant technology will continue to improve the safety and quality of collagens used in artificial corneal substitutes.

4. CURRENT TRENDS IN CORNEAL APPLICATIONS IN REGENERATIVE MEDICINE

The treatment methods of corneal defects vary depending on the severity of the defect. Antibiotics, different ointments and tissue glues are some of the cures for minor ulcerations, while the most serious corneal defects may require PK, deep anterior lamellar keratoplasty (DALK) or artificial corneal substitutes. In the following chapters, these methods will be discussed along with the latest trends in modern regenerative medicine in corneal applications.

4.1 Contemporary treatments and clinical applications for corneal defects

Keratoplasty

Keratoplasty is a surgical operation in which a damaged cornea is replaced with an allogenic transplant. Depending on the severity of the defect, keratoplasty can be either lamellar, with only a layer of the cornea replaced, or penetrating, in which the whole cornea is received from a donor (Al-Yousuf et al., 2004).

However, the demand for donors and good quality tissue surpasses their availability in many countries, which creates an increasing need for artificial corneal substitutes (Griffith et al., 2009; Ghezzi et al., 2015). Moreover, the relatively common problems that can occur among corneal transplants, such as immunological rejection, infections and inflammations, further increase the number of operations needed with corneal transplants. Even after a successful keratoplasty, the symptoms of rejection can cause severe and long-lasting discomfort for the patient, which can lead to the need of regrafting (Al-Yousuf et al., 2004; Griffith et al., 2009; Ghezzi et al., 2015).

Synthetic corneal substitutes

A more advanced, although only provisional, solutions are fully synthetic corneal substitutes known as keratoprostheses (KPros). KPros are often used when traditional keratoplasty cannot be performed, having the main purpose of helping the patient to recover a functional level of eyesight rather than actually healing the damaged cornea. (Griffith et al., 2009)

Rather than being biodegradable, KPros are normally made from tissue-friendly, non-biodegradable plastics combined with bio-inert metals like titanium (Griffith et al., 2009; Ghezzi et al., 2015). They are designed to have a clear centre with a porous perimeter that ensures attachment to the eye surface through fibroblast ingrowth. It is essential that the

synthetic materials used for KPros do not cause any adverse tissue effects that might decrease the tissue acceptance of the implant. To improve their biocompatibility, the most recent models of KPros utilise ECM components on their surfaces to enhance implant anchoring, as well as new kinds of materials to boost the nutrient and oxygen permeability of the implants. (Griffith et al., 2009)

Amniotic membrane

Amniotic membrane (AM) gained increasing attention as an option for treating conjunctival ulcers in the 1940s, but its use was discontinued at that time due to the lack of sufficient surgical techniques. However, with the development of modern methods of microsurgery and tissue engineering, AM has been brought back into use as a substrate for ocular reconstruction and as an ocular plaster to enhance wound healing. (Kruse et al., 1999)

The most important reasons for the use of the AM in regenerative medicine are its anti-inflammatory and wound healing properties. It has been used both on its own to help healing and stabilising the corneal tissue after injuries, as well as accompanied with limbal allografts to improve the outcome of the transplantation (Tseng et al., 1998). In their study, Tseng *et al.* (1998) tested the performance of the AM in these two cases in patients with different degrees of LSCD. The patients with moderate (5 patients, 7 eyes) or severe (13 patients, 14 eyes) limbal deficiency received both AM and allograft limbal transplantation, while the patients with mild limbal deficiency (9 patients, 10 eyes) only received an AM transplantation. The results showed that the AM on its own is enough to heal the corneal surface and improve the vision in patients with only partial limbal deficiency, and combined with allogenic limbal transplant, able to enhance the success of the transplantation. However, in the most severe cases of LSCD Tsung *et al.* found the tested methods with the AM insufficient, and that a PKP operation would need to be included for eyesight recovery.

Although the AM has shown to be a potential substrate for corneal surface regeneration, the use of synthetically produced biomaterials would be a better option from the material aspect. Due to its natural origin, the properties of the AM cannot be specifically tailored nor homogeneity guaranteed. AM is not readily available and there is a possibility for immunological reactions. (Hopkinson et al., 2006)

4.2 Current focus of research in corneal regenerative medicine

Recent methods in the treatment of corneal defects utilise the techniques of modern regenerative medicine, aiming to improve tissue growth through biodegradable implants, incorporated cells and growth factors combined with materials that mimic the features of the natural cornea. The regeneration of healthy tissue with minimal invasiveness and optimal biocompatibility of materials is a goal that researchers in this field pursue, and which novel corneal substitutes aim for using both synthetic and natural materials.

Many natural polymers have been studied for corneal applications. Apart from hyaluronan and collagen, some examples are silk fibroin (e.g. Lawrence et al., 2009; Liu et al., 2012; Hazra et al., 2016), alginate, chitosan (Liang et al., 2011) and gelatin (Tonsomboon et al., 2013). The use of natural materials has been both promising and problematic. Natural polymers are mostly non-toxic and can be processed in mild conditions, which improves their tissue-friendliness, but on the other hand materials that do not naturally occur in the host tissue have the possibility of provoking serious immunological problems.

To overcome biocompatibility and quality issues, large effort is currently put into the production of natural polymers through recombinant DNA (rDNA) technology, which makes it possible to produce biopolymers in the laboratory without the danger of transferring pathogens or encountering inconsistencies in the quality. Through genetic engineering, rDNA technology aims to synthesize a desired product, such as collagen, in a host cell by modifying its DNA with sequences taken from two or more external sources. Sources to produce recombinant collagens can be bacteria, mammalian and plant cells, as well as silk worms or even transgenic tobacco. (Liu et al., 2008)

Some research groups (Gaudreault et al., 2003; Guo et al., 2007; Proulx et al., 2010) have concentrated an approach known as self-assembling corneal substitutes, with the principle of letting cultured cells produce their own scaffold through the secretion of ECM products and macromolecules. Proulx *et al.* induced the production of collagen in dermal fibroblasts via the addition of ascorbic acid. The collagen produced by the cells was collected in the form of thin sheets, which were then stacked together to reproduce an arrangement resembling the lamellar structure of the native corneal stroma. On both sides of this artificial stroma, Proulx *et al.* seeded an endothelial and an epithelial cell layer, which was stratified by culturing the cells at air-liquid interface. The stratification of the epithelium was confirmed by identifying positive keratin 3 markers, which indicate a successful epithelial differentiation. In this stromal construct, all three corneal cell types – epithelial, stromal, and endothelial – were seeded. The resulting self-assembled cornea had similar optical characteristics to the natural cornea, and was fully free of any non-biological materials. The drawbacks of this technique, as summarised by Griffith *et al.* in their review on corneal substitutes (2009), are the slowness of the production and the almost certain need to use the receiver's autologous cells, which further lengthens the process of implant manufacturing.

5. ARTIFICIAL CORNEAS – CLINICAL OUTCOMES AND FUTURE PERSPECTIVES

Hydrogel materials have been a point of interest for corneal applications due to their aqueous 3D structure, highly modifiable properties and easy manufacturing and shaping. Currently, there are only few artificial corneas in clinical use, namely the Boston KPro, the AlphaCor® and the osteo-odonto-keratoprosthesis (OOKP), of which only the AlphaCor® is made of a hydrogel material. Although most hydrogel corneal substitutes are still at the preclinical stage, new solutions are constantly emerging and proceeding towards clinical trials. In this chapter, the current commercial status and future prospects of artificial corneas are briefly discussed.

The most widely used hydrogel corneal substitute is the AlphaCor®, previously known as the Chirila Keratoprosthesis, a device manufactured from synthetic poly(2-hydroxyethyl methacrylate) (PHEMA), and is currently the only hydrogel-based corneal substitute in commercial use. The AlphaCor® received the approval by the Food and Drug Administration (FDA) in 2002 and has proved to be a suitable option for patients with multiple failed corneal grafts or other serious complications that have made further grafting impossible. The implant is composed of a core optics and a porous skirt for tissue integration, and utilises interpenetrating polymer network (IPN) technology in the connection between its rigid core and porous skirt. This interesting design is based on the different types of behaviour of PHEMA depending on its water-content: the core of the AlphaCor® is manufactured from PHEMA with < 40% water-content, forming a clear, homogenous and mechanically robust hydrogel, while the skirt is prepared with a higher water-content, which results in a microporous, spongy gel. (Myung et al., 2008)

In their review article, Myung *et al.* (2008) state that in successful cases, AlphaCor® has shown one-year retention rates of approximately 80 %, providing good eyesight performance. Due to its lack of metal components, the AlphaCor® also has a more pleasant cosmetic appearance compared to the Boston KPro, for example. However, unlike the Boston KPro, the AlphaCor® requires a two-step implantation procedure, with the optics being exposed only after the second stage. Another drawback of the AlphaCor® is that PHEMA as a material cannot maintain a sufficient water content for the diffusion of nutrients to be efficient, which is why the AlphaCor® does not support the development of an epithelial cell layer on its surface (Myung et al., 2008). Referring to a review by Carlsson *et al.* (2003), Myung *et al.* state that epithelial overgrowth has been found essential to prevent external particles and bacteria from contaminating the cornea due to the natural cellular barrier, resulting in less post-surgical complications. Therefore, epithelialisation is an important aspect in the development of artificial corneas today. (Myung et al., 2008) The Boston KPro, despite classified as an artificial cornea, requires a corneal graft from

a donor. This removes the problem of a missing epithelium, but involves risks of rejection or transferring of pathogens, similarly to a keratoplasty.

Research in the field of corneal implants is thriving, and new alternative KPros are emerging, such as the KeraKlear® and the Miro Cornea®. Although only preliminary results from clinical trials have been reported, these devices have shown potential to rival the Boston KPro and the AlphaCor® as artificial corneal substitutes in the near future. Both products physically resemble soft contact lenses, and are manufactured from different acrylic-based biocompatible polymers. The Miro Cornea® is coated with genetically engineered fibronectin to enhance its integration into the surrounding tissue (Duncker et al., 2014). In a clinical study by Duncker *et al*., the Miro Cornea® was implanted into the eyes of four patients with corneal blindness, resulting in good tissue integration and stability during a 20–52-month follow-up period. Like the AlphaCor®, The KeraKlear® has a single-piece core-and-skirt design, with 18 holes around its periphery to maintain tissue integration. Although some difficulties in implantation have been reported (Shrage et al., 2014), it has already obtained the European CE marking, but is yet to receive the FDA approval for the U.S. market. Preliminary results for both newcomers are promising, but Shrage *et al.* conclude that more extensive clinical trials are still necessary to evaluate their long-term performance.

Most of the artificial corneas are based on acellular scaffolds made of biocompatible polymers. However, contemporary research is getting more focused on the self-assembly approach, as briefly discussed in Chapter 4.2. Recently many biomaterials and tissue engineering groups have been developing artificial corneas by inducing the cells to create their own ECM through the addition of different growth factors or other biomolecules. For example, by adding ascorbic acid in the cell suspension, Proulx *et al.* (2010) activated the production of collagen, which was then harvested and built from thin sheets into a multilayer scaffold. Apart from being tissue-friendly, this approach essentially removes the risk of pathogen transfer, which is often present when using collagen or other natural polymers from external sources.

More recently a wider range of biomolecules have been used in self-assembling artificial corneas. Islam *et al.* (2016) recognised problems with the insufficient mechanical strength of self-assembled collagen scaffolds, and instead used smaller units known as collagen-like peptides (CLP). The principle of using CLPs, as described by Islam *et al.*, is in their ability to form collagen-like nanofibres with triple-helical structures, which can function as physical crosslinks in polymer systems or as 3D scaffolds on their own. As the basis for their study, Islam *et al.* used an article by O'Leary *et al.* from 2011, who used a peptide of 36 amino acids that mimicked collagen fibrils. However, the method was modified by adding a glycine spacer and an extra cysteine, which enabled covalent bonding with a branched PEG-maleimide polymer, which in turn was based on methods described by Perez *et al.* in 2011. Through this combination, Islam *et al.* could make the mechanical resilience of the hydrogel sufficient for surgical handling, describing the result as a good

combination of rigidity and flexibility. The materials were moulded into corneal shape and implanted in four mini-pigs by anterior lamellar keratoplasty. At 12 months after implantation, the eyes had remained stable and transparent apart from a mild haze in the implant-host interface. Showing similar morphology to the unoperated healthy eyes, stromal tissue had grown inside and epithelial tissue on the surface of the implant. Additionally, noticeable ingrowth of corneal nerves along with previously absent collagen I and V could be found inside the implants, indicating good host response and tissue integration. (Islam et al., 2016)

With the intense research going on in corneal tissue engineering, novel solutions are frequently discovered and new clinical data obtained from different types of designs. Following the path of pioneering products such as the AlphaCor®, hydrogel implants are still gaining increasing interest due to their cornea-like properties and great variety of features. In the pursuit of cornea-mimicking features, self-assembling and recombinant biopolymers are showing the way for a very promising future in the field of corneal implantology.

6. AIM OF THE THESIS

The overall purpose of this thesis was to develop a hydrogel material with controlled and defined properties that could provide a suitable platform for corneal cell proliferation and differentiation, while meeting the mechanical and optical properties required for such application. Similar methods and materials have been described in multiple publications, but the basis for the polymers and gels prepared in this study is in the research done by Paul Bulpitt *et al.* in 1999, and O.P. Oommen and his group in 2013, who prepared gels from similarly modified hyaluronan components. The novelty value of this study comes from the incorporation of collagen into the hydrazone crosslinked HA structure and the wide range of characterisation methods used to study them.

The main goals set for this Master's thesis were:

1. To develop a hydrazone-crosslinked hyaluronan hydrogel with optical functionality and suitable properties for corneal cell culturing and surgical application.
2. To characterise the developed materials, with the focus being on their mechanical, viscoelastic and optical properties as well as hydrolytic stability and swelling kinetics.
3. To compare the prepared hydrogels to similar materials found in literature, and to evaluate their potential to be used for corneal regeneration.

The material development involved characterisation of the viscoelastic, mechanical and optical properties of the hydrogels, along with their swelling kinetics, stability and behaviour under air exposure. The mechanical properties of the hydrogels were measured using compression testing equipment, and their viscoelastic behaviour was tested in a cone-plate rheometer. Hydrogel transparency and refractive indices were determined using a fibre spectrometer and surface plasmon resonance equipment with customised test protocols.

If a potential material filled the mechanical and optical requirements sufficiently, it continued to cell viability testing. The cell culture tests were conducted by the Eye Group of BioMediTech in Tampere, Finland, which is why the tests will not be discussed in greater detail within this thesis. However, the cell tests guided the development of the materials throughout the process, and often determined which material properties required improving and which gel formulations were to be developed further.

EXPERIMENTAL PART

7. MATERIALS AND METHODS

7.1 Materials

Hyaluronic acid sodium salt from streptococcus equi (M_w 1.5×10^5 g/mol) was purchased from Lifecore Biomedical (Chaska, MN, USA). Adipic acid dihydrazide (ADH, M_w 174.20 g/mol) and hyaluronidase (HAse) enzyme from bovine testes (type I-S, 400–1000 U/mg) were purchased from Sigma Life Science (St. Louis, MO, USA). Sodium periodate, dimethyl sulphoxide (DMSO), ethylene glycol and 1-Ethyl-3-[3-(dimethylamino)propyl]-carbodiimide (EDC) were purchased from Sigma-Aldrich (St. Louis, MO, USA). 1-hydroxybentzotriazole (HOBt), 3-amino-1,2-propanediol and carbodihydrazide (CDH, M_w 90.08 g/mol) were purchased from Aldrich (St. Louis, MO, USA). Dialysis membranes (Spectra/Por cut-off 3500, 12–14 000 and 25 000 g/mol) were purchased from VWR International (Radnor, PA, USA). Collagen I used in the study was secreted from rat tails by a collaborating research group. Sodium chloride (NaCl), disodium phosphate (Na_2HPO_4) and sodium dihydrogen phosphate monohydrate ($NaH_2PO_4 \cdot H_2O$) used for PBS preparation were purchased from J.T. Baker® (Avantor Performance Materials, Center Valley, PA, USA). Dulbecco's Modified Eagle Medium was purchased from Gibco® (Thermo Fisher Scientific, Waltham, MA, USA). All solvents used in the study were of analytical quality. Milli-Q water was used in the syntheses and analyses.

7.2 Modification of hyaluronan

7.2.1 Syntheses of aldehyde-modified hyaluronans

HA-ALD1 component

The first aldehyde modification of hyaluronan (HA-ALD1) was carried out following a protocol reported by Jia *et al.* in their article (2006), from which a more detailed description can also be found. The goal for the modification was to form dialdehyde groups on the glucuronic acid moiety of the HA through periodate oxidation of its C2–C3 vicinal diols.

Aqueous solutions of the HA periodate were mixed by adding the periodate drop-by-drop in room temperature, followed by mixing for four hours in the dark. Any unreacted periodate was inactivated by adding ethylene glycol and stirring for another hour. The solution was then exhaustively dialysed against dH_2O for three days, after which it was freeze-dried to obtain the final HA-ALD1 product.

HA-ALD2 component

The HA-ALD2 component was prepared as reported by Martínez *et al.* (2011). The procedure involved two stages: the first one involved a diol modification of the HA, followed by a selective oxidation of its diol groups into aldehyde functionalities in the second phase.

First, the hyaluronic acid was dissolved in distilled water, followed by the addition of 3-amino-1,2-propanediol and HOBt, which was pre-dissolved in 1:1 volume mixture of acetonitrile and water. The pH was adjusted to 6.0 with 1 M HCl, EDC was added and let to stir overnight, after which the solution was dialysed for 24 hours against dilute HCl (pH = 3.0) containing 0,1 M NaCl, using a 3500 g/mol cut-off membrane. At this point the first product, the diol-modified HA, was lyophilised.

The synthesis of the HA-ALD2 derivative initiated by dissolving the first phase product in distilled water. Sodium periodate ($NaIO_4$), pre-dissolved in water, was added and let to stir for 5 minutes before ethylene glycol was added to quench the excess periodate. The solution was stirred for 2 hours and then dialysed (3500 g/mol cut-off membrane) for 24 hours against distilled water. The final product was lyophilised and stored in a refrigerator.

7.2.2 Syntheses of hydrazide-modified hyaluronans

HA-ADH component

The ADH-modified hyaluronan component (HA-ADH) was prepared as described by Karvinen *et al.* (2017). The modified hyaluronan was created through the reaction of the carboxylic groups in its glucuronic acid element with and excess of adipic acid dihydrazide.

The preparation started with dissolving sodium hyaluronate in distilled water overnight in a 100-ml three-neck flask. The following day a 30-fold molar excess of ADH was added, the pH was adjusted to 6.8 using 0.1 M NaOH or 0.1 M HCl and the system was connected to N_2 atmosphere. HOBt and EDC were mixed together inside a glove box, dissolved in 1:1 (volume) DMSO/H_2O and added to the mix. The pH was maintained at 6.8 and the reaction was let to proceed overnight. The following day the pH was set to 7.0 and the solution was dialysed for 3–5 days against distilled water with a 12–14 kDa MW cut-off membrane, after which the product was precipitated by adding NaCl and ethanol. Lastly, the HA-ADH precipitate was gathered, dissolved in water, freeze-dried and stored in a refrigerator.

HA-CDH component

The CDH-modified hyaluronan component was prepared per the method presented by Oommen *et al.* (2013), and has a similar protocol to the previously presented ADH-modification of hyaluronan. The main purpose of the modification was to make the carboxylic

groups in the HA react with an excess of carbodihydrazide in the presence of EDC and HOBt.

The modification process began with dissolving 1 mmol of disaccharide repeat units of HA in distilled water and connecting the flask in N_2 system. This was followed by the addition of the CDH and HOBt and adjusting the pH to 4.7 with 0.1 M NaOH of HCl. The EDC was weighed inside a glove box and added into the flask. The solution was mixed and left to proceed overnight. The following day the mixture was dialysed for 48 hours against dilute HCl (pH = 3.5) containing 0,1 M NaCl, using a 3500 Da cut-off dialysis membrane. The resulted product was freeze-dried and stored inside a refrigerator.

7.3 Preparation of hydrazone-crosslinked hyaluronan hydrogels

Two different aldehyde and hydrazide modifications were done to the hyaluronan components. The modifications were based on four different literature references with minor alterations. The hyaluronan derivatives with different modifications were named as shown in Table 7.1 below. Additionally, the non-collagenous and collagenous gel versions were distinguished with suffixes 1 and 2, in respective order.

Table 7.1. *Gel component abbreviations and their descriptions.*

Type	Abbreviation	Description	Reference
A	HA-ALD1	Aldehyde-modified hyaluronan derivative.	Jia, 2006
	HA-ADH	Hydrazide-modified hyaluronan derivative, ADH modification.	Karvinen *et al.*, 2017
B	HA-ALD2	Aldehyde-modified hyaluronan derivative.	Martínez *et al.*, 2011
	HA-CDH	Hydrazide-modified hyaluronan derivative, CDH modification.	Oommen *et al.*, 2013

To find the optimal component concentrations and ratios for the gels, a total of 20 different gel compositions were tested. The main properties observed during the preparation of different gels were the gelation speed and quality, the transparency and the mechanical stiffness of the gel. The mechanical rigidity was evaluated knowing the fact that the final products would need to withstand surgical handling without breaking or deforming. The variable parameters, such as different solvents, gelation platforms, component concentrations and volume ratios were changed according to the results of the previous iterations. A list of all the tested gel formulations can be found in Table 7.2 below.

Table 7.2. *A summary of gel formulations in the optimisation phase. The aldehyde derivatives are titled A) HA-ALD and the hydrazide-modified components B) HA-HY. Values in parentheses indicate the polymer concentrations in milligrams per millilitre [mg/ml].*

	Formulation			**Component amount (µl)**			**Component solution W = Water P = PBS**		
#	**A) HA-ALD**	**B) HA-HY**	**C) Collagen**	**A**	**B**	**C**	**A**	**B**	**C**
1	**HA-ALD1 (20)**	**HA-ADH (10)**	**-**	**50**	**50**	**-**	**W**	**W**	**-**
2	HA-ALD1 (20)	HA-ADH (10)	-	50	50	-	P	P	-
3	HA-ALD1 (20)	HA-ADH (10)	RAT (2)	50	50	25	W	W	Acetic acid
4	-	-	RAT (2)	-	-	200	-	-	Acetic acid
5	HA-ALD1 (25)	HA-ADH (12,5)	RAT (2)	50	50	25	W	P	Acetic acid
6	HA-ALD1 (25)	HA-ADH (12,5)	RAT (2)	50	50	25	W	1:2 WP	Acetic acid
7	HA-ALD1 (25)	HA-ADH (12,5)	RAT (2)	50	50	25	W	1:1 WP	Acetic acid
8	HA-ALD1 (20)	HA-ADH (10)	RAT (2)	50	50	25	W	1:1 WP	Acetic acid
9	HA-ALD1 (25)	HA-ADH (12,5)	HUMAN (1)	50	50	25	W	1:1 WP	Acetic acid
10	HA-ALD1 (20)	HA-ADH (10)	HUMAN (1)	50	50	25	W	1:1 WP	Acetic acid
11	HA-ALD1 (25)	HA-ADH (12,5)	HUMAN (1)	50	50	50	W	1:1 WP	Acetic acid
12	HA-ALD1 (22,5)	HA-ADH (11,25)	-	50	50	-	W	1:1 WP	-
13	HA-ALD1 (22,5)	HA-ADH (11,25)	HUMAN (1)	50	50	25	W	1:1 WP	Acetic acid
14	HA-ALD1 (22,5)	HA-ADH (11,25)	HUMAN (1)	50	50	50	W	1:1 WP	Acetic acid
15	**HA-ALD1 (22,5)**	**HA-ADH (11,25)**	**RAT (2)**	**50**	**50**	**25**	**W**	**1:1 WP**	**Acetic acid**
16	HA-ALD1 (22,5)	HA-ADH (11,25)	RAT (2)	50	50	50	W	1:1 WP	Acetic acid
17	HA-ALD2 (20)	HA-CDH (20)	HUMAN (1)	50	50	50	W	1:1 WP	Acetic acid
18	**HA-ALD2 (30)**	**HA-CDH (30)**	**RAT (2)**	**50**	**50**	**25**	**P**	**P**	**Acetic acid**
19	HA-ALD2 (30)	HA-CDH (20)	HUMAN (1)	50	50	50	P	P	Acetic acid
20	**HA-ALD2 (30)**	**HA-CDH (30)**	**-**	**50**	**50**	**-**	**P**	**P**	**-**

Through this type of iteration, the optimal gel compositions were determined and four different gels were chosen for further characterisation from each gel type: One collagenous gel and one control gel without collagen. These four gel formulations are emphasised in bold in Table 7.2.

Therefore, the following four gels continued to the characterisation phase:

A1: HA-ALD1 (20) + HA-ADH (10)
A2: HA-ALD1 (22.5) + HA-ADH (11.25) + Rat tail collagen I (2)
B1: HA-ALD2 (30) + HA-CDH (30)
B2: HA-ALD2 (30) + HA-CDH (30) + Rat tail collagen I (2).

As seen from Table 7.2, the optimal component ratios were 1:1 for gels A1 and B1, and 2:2:1 for the gels A2 and B2, with collagen as the smallest ratio. The optimal mixing order of components was 1. HA-HY 2. Collagen 3. HA-ALD, since it was found that the mixing of collagen and the aldehyde modified hyaluronan caused the mixture to gelate, while a collagen-HA-HY solution remained liquid. This was presumed to be caused by the linking of the amino groups of the collagen molecules with the aldehyde groups of HA-ALD1 and HA-ALD2 derivatives, which resulted in premature crosslinking.

For hydrogel preparation, the polymer components were dissolved in distilled water or in filtered PBS (pH = 7.4). Since no additional crosslinking agents were needed, the gels were prepared simply by mixing the aldehyde and the hydrazide components together. As mentioned above, in gels A2 and B2 the collagen solution was added to the hydrazide-modified hyaluronan component before adding the aldehyde component. The gelation was done in an incubator at 37 ºC for 1 h. The determination of gelation speed was done using the so-called tube tilt test (ASTM International, 2011), in which the gel is prepared in a tube and tilted at different time points to determine when the gelation takes place. The recorded gelation time was the point at which the liquid stopped flowing as the tube was tilted.

The gels tested with collagen I from human placenta performed poorly in cell culture tests, which is why their testing was discontinued. It appeared that the cells did not remain viable in the presence of the human collagen I, although no definite reason for this was found. A possible cause for this result could have been the low pH of the mild acetic acid solution of the human collagen I, or inconsistencies in its quality.

7.4 Hydrogel characterisation

The properties of the hydrogels were characterised using a variety of test methods. Characterised properties involved mechanical, chemical, optical and stability tests, as well as the evaluation of degradation and swelling behaviour in cell culture medium. Different material characterisation methods used for this thesis are summarised in Table 7.3 below.

Table 7.3. *An overview of the material characterisation methods used in this study.*

Characterisation	**Method**
Mechanical properties	*Compression test*
Viscoelastic properties	*Cone and plate rheometry*
Polymer chemical structure	*Fourier transform infrared spectroscopy (FTIR)*
Optical properties	*Refractive index (RI) measurement & fibre spectrometer*
Swelling kinetics	*Swelling Ratio measurement*
Enzymatic degradation	*Degradation by bovine testicular hyaluronidase*
Air exposure behaviour	*Cell culture inserts in a customised well plate*

7.4.1 Chemical structure

The chemical compositions and the success of polymer modifications were verified using Fourier transform infrared spectroscopy (FTIR). One sample (*V=100 µl, n=1*) of each polymer component and of each gel was prepared in cut 1 ml syringes and lyophilised before testing. The samples in the FTIR measurements are presented in Table 7.4.

Table 7.4. *Components and gels characterised in the FTIR measurements.*

Aldehyde modified hyaluronans:	HA-ALD1, HA-ALD2
Hydrazide modified hyaluronans:	HA-ADH, HA-CDH
Collagen:	Rat tail collagen I
Hydrogels:	HA-ALD1 (20) + HA-ADH (10)
	HA-ALD1 (22.5) + HA-ADH (11.25) + Rat collagen I (2)
	HA-ALD2 (30) + HA-CDH (30)
	HA-ALD2 (30) + HA-CDH (30) + Rat collagen I (2)

The testing was done at the Department of Chemistry and Bioengineering of Tampere University of Technology using a Spectrum One FT-IR Spectrometer (PerkinElmer, Waltham, MA, USA) with Attenuated total reflection (ATR) sampling technique within 650 to 4000 cm^{-1} wavelength range (0.5 to 64 cm^{-1} respective resolution).

7.4.2 Mechanical and viscoelastic properties

Compression tests

The mechanical properties of the hydrogels were tested using a unidirectional, unconfined compression test at room temperature (r.t.) in air atmosphere. The compression tests were performed with BOSE Biodynamic Electroforce Instrument 5100 (Bose Corporation, Eden Prairie, MN, USA) equipped with a 225 N load cell, flat platens and a Wintest 4.1 testing software. The platens were covered with Parafilm® and wet tissue paper to avoid sample drying and to hold the samples in place. A constant strain rate of 0.1 m/min (0.1666 mm/s) was used, and the compression was continued up to 70–75 % of maximum compressive strain. Examples of the compression test samples can be seen in Figure 7.1 below.

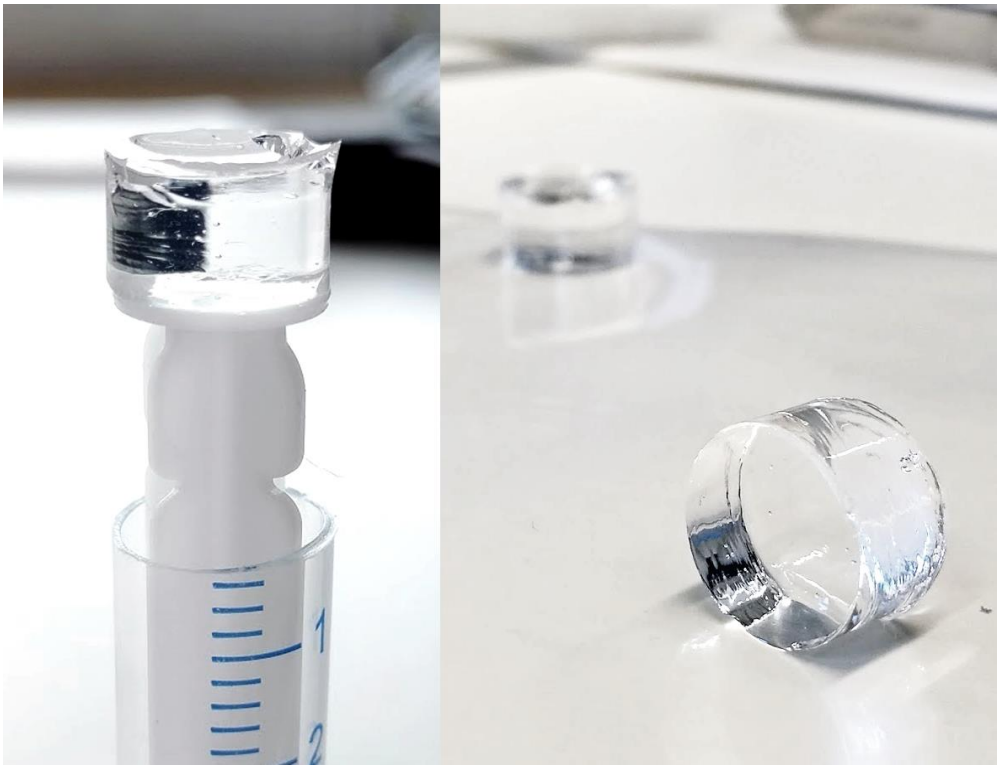

Figure 7.1. *Cylindrical samples (V = 875 µl) for the unconfined compression testing were prepared in cut 5 ml syringes.*

The samples (*V = 875 µl*, *n* = 5) were prepared in 5 ml cut syringes, which were closed using Parafilm® and gelated at 37 ºC for a minimum time of 1 h. Prior to the measurement, the samples were let to stand in room temperature for 24 hours after gelation to ensure gel uniformity. After removal from the syringe, the sample dimensions were measured

using a digital vernier caliper. For each sample, the displacement and the scan time (= displacement divided by compression speed) were calculated according to sample dimensions. For each sample, the number of data collection points, or scan points, was determined as the scan time multiplied by four.

Through mechanical testing, it is possible to determine a solid material's modulus from the slope of the linear elastic region of its stress-strain curve, which obeys Hooke's law. However, because of the characteristic non-linear behaviour of hydrogels, the law does not apply other than at very low strain values. Instead, the values for so-called stiffness and second-order elastic constants were calculated for the hydrogels in this study, using the following methods described by Karvinen *et al.* (2017).

Stiffness was defined as the derivative of stress with respect to strain, which in turn is the second derivative of energy density with respect to strain. The measured stress and strain values can be presented as the values of elastic constants using the following polynomial function:

$$\sigma(\varepsilon) = \sum_{k=0}^{n} c_k \varepsilon^k, \tag{1}$$

where σ is the stress, ε is the strain, and the coefficients c_k are the elastic constants of the material. Consequently, the stiffness can be defined as

$$\frac{d\sigma}{d\varepsilon} \equiv \tau(\varepsilon) = \sum_{k=1}^{n} k c_k \varepsilon^{k-1}, \tag{2}$$

in which the value of c_k is the *second-order* elastic constant (c_{k-1} would be the k^{th}-order elastic constant). To generate the stiffness-strain curve, a 6$^{\text{th}}$-degree polynomial function was fitted with the stress-strain graph of each sample, and the stress σ values were plotted as a function of strain ε. In other words, by plotting the stress-strain function (1) with the measurement data using the value $n = 6$ in the equation (1). The second-order elastic constants for each gel type were then calculated from the average stiffness-strain curves of parallel samples at 0–0.15 strain range by finding the stiffness value with the smallest relative standard deviation i.e. the smallest ratio between the standard deviation and its corresponding mean average stiffness value. The comparison between the stiffness functions $\tau(\varepsilon)$ of different gels was done using polynomial (2) by plotting the stiffness τ values from equation (1) as a function of strain. (Karvinen et al., 2017)

Cone and plate rheometry

The viscoelastic properties of the gels, such as the dynamic shear moduli, were evaluated in a Haake RheoStress RS150 rheometer with a RheoWin 4.3 software (Thermo Fischer Scientific, Waltham, MA, USA) in the material characterisation laboratory of the Department of Materials Science in TUT. Cone and plate geometry (Type: 222-0598, cone angle = 1 º, diameter = 20 mm, gap = 0.8 mm) was utilized for all tests at a constant temperature of 37 ºC. The samples ($V = 500\ \mu l$) for frequency sweep ($n = 3$) and amplitude sweep ($n = 3$) measurements were prepared in 20 ml cut syringes, made airtight with Parafilm® and gelated at 37 ºC for 1 hour. The measurements were conducted 24 hours after the gelation.

Amplitude sweeps ($\gamma = 0.01–10$, *constant* $\omega = 1$ *Hz*) were used to determine the linear viscoelastic region (LVR) of the gels, while the storage moduli *G'* and loss moduli *G''* were measured using frequency sweeps (*constant* $\gamma = 0.1$ *(based on LVR),* $\omega = 0.1\text{-}10$ *Hz*). The measurements were controlled and the data collected with Haake Rheowin 4 software. The collected rheometer data included the values for frequency, strain, storage and loss moduli, phase angle delta (δ) and tan δ. The tan δ expresses the internal friction of the material through the relationship between the loss and the storage modulus: $tan\,\delta = G''/G'$. The strength of the hydrogel structure can be estimated using this value: if the measured tan δ < 0.1 the gel can be considered strong, and if tan δ > 0.1 the gel has a weak structure.

7.4.3 Optical properties

Refractive index

The optical properties of the gels were evaluated by measuring their refractive indices and transparency. The RI of each gel type was determined with a surface plasmon resonance equipment Navi 210A (BioNavis, Tampere, Finland).

The device includes a goniometer and a laser light source, with which the sample surface can be scanned from different angles to determine its critical angle of total internal reflection. Different lasers were used, but all the calculations were done using 670-nm wavelength. For the measurement, the procedure was modified so that no gold-plated sensor slide was used in the flow cell – as in an SPR measurement – but instead a glass sensor slide without any metal coating. The sensor slide, made of BK7 glass with a known RI, was used for device calibration before the measurement. In the calculations, a general RI value of n_{glass} = 1.514 was used, based on a literature value given for BK7 glass at 670 nm wavelength (Nakajima, 2015). After calibration, a sufficient amount of gel was applied on the flow cell to fill it thoroughly, and the flow cell was then tightened against the glass sensor slide as in the normal procedure.

From this measurement, a curve of internal reflection for each sample was obtained, showing the reflection coefficient as a function of angle of incident, as will be presented

in Chapter 8.4.1. The RIs of the gels were determined from the curves utilizing equation (3) derived from Bragg's law:

$$n_{gel} = n_{glass} \times \sin \alpha, \quad (3)$$

where n_{gel} and n_{glass} are the refractive indices of the hydrogel and the sample slide, and α is the value of the angle of incident determined from the curve transformed into radians.

Transparency

Transparency of the hydrogels was evaluated visually during the optimisation phase. However, between different publications no widely-used or standardised protocol for measuring hydrogel transparency could be identified. To approach this problem, the principle for a fibre spectrometer-based transparency testing method was developed as a part of this study. Even though in the scope of this thesis it was not possible to optimise the design and the testing protocol, the development this far will be described and discussed in the following paragraphs.

The equipment for the transparency measurements consisted of a custom-fabricated sample holder and a JAZ spectrometer equipped with model QP400-1-UV-VIS fibre and a sample holder mount (Ocean Optics, Dunedin, FL, USA). The data was collected and processed using the related OceanView computer software. The mount and the optical fibre are shown in Figure 7.2.

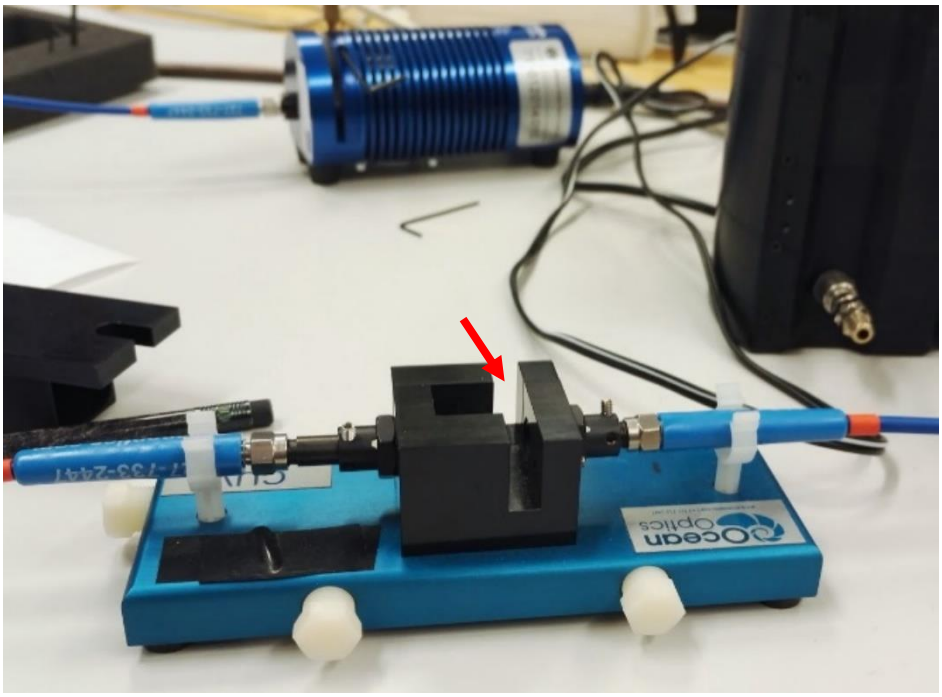

Figure 7.2. *Fibre spectrometer equipment used in the hydrogel transparency measurements. The sample holder is placed vertically in the gap indicated by the arrow, where the light beam passes through it horizontally.*

The custom sample holder consisted of two standard microscopy slides and a piece of polydimethylsiloxane (PDMS) membrane (*thickness = 800 µm*) that was used to create wells to hold the gel samples. The design process started from defining the main requirements for the transparency measurement method, which included test repeatability, acquisition of numeric output data, and the possibility to test samples with similar dimensions to the native cornea.

The standard samples used for the fibre spectrometer measurements are normally prepared in cuvettes of 1–2 ml. Due to the material costs of the gels and to the inconvenient sample thickness for this purpose, a different sample holder needed to be made. Multiple designs were tested and further improved based on the results.

To mimic the dimensions and shape of the cornea, thin hydrogel discs of a definite diameter were to be prepared on a microscopy slide. This way the transparency could be measured through the glass and the hydrogel, using a clean spot of the same microscopy slide as the reference value and in device calibration. The diameter of the gels was controlled by using a punch tool with 10 mm diameter to make holes on the PDMS film and attaching it on the surface of the microscopy slide. The membrane would self-attach on the glass surface as it was placed there, after which the gels were prepared in the wells formed by the bottom glass and the PDMS walls. To ensure uniform sample thickness, another microscopy slide was attached on the opposite side so that the PDMS film and the samples would remain compressed between the two glasses. An illustration of the sample holder used in the measurements is presented in Figure 7.3 below.

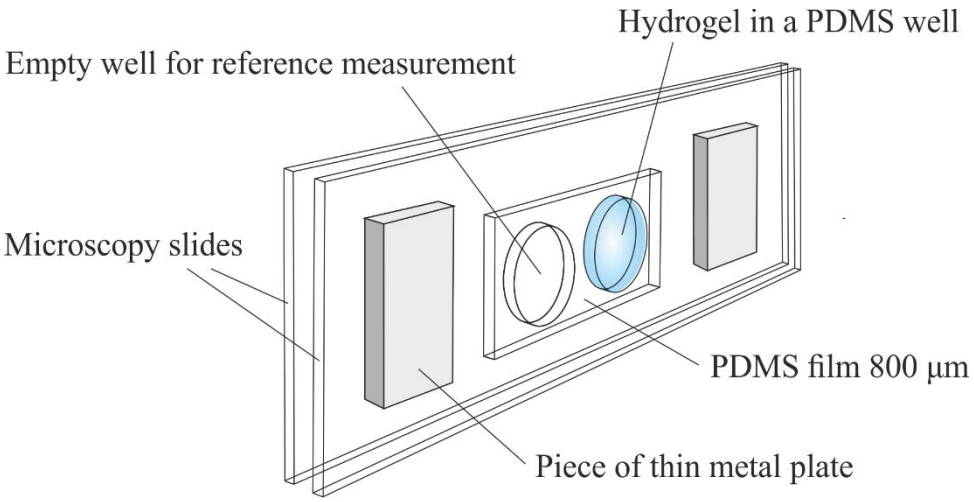

Figure 7.3. *Illustration of the custom-fabricated sample holder for fibre spectrometer, used in hydrogel transparency measurements.*

As will be described further in the results section, the design functioned well in principle, but would need some improvements with ensuring the parallelism of the microscopy slides and with securing the sample holder system on the spectrometer. Most of the inconsistencies in the results were concluded to be caused by light reflection and scattering caused by the wrong alignment of the microscopy slides.

7.4.4 Swelling behaviour

The swelling of different gel types was evaluated in an experiment where the samples were immersed in DMEM/F-12 cell culture medium in 15 ml Falcon® tubes at 37 ºC. The swelling behaviour was observed during a period of 48 hours.

The experiment was carried out with lyophilised hydrogel samples and with 'fresh' gels that were prepared one hour before the experiment. Three parallel samples ($V = 125\ \mu l$, $n = 3$) of each gel were immersed in the medium and weighed at time points of 0, 1, 2, 4, 6, 24 and 48 hours. A laboratory balance with 1 mg resolution was used for the swollen and fresh gels, while the lyophilized dry samples were weighed using an analytical laboratory balance with 0.01 mg resolution. A photograph of a gel B1 sample prior to its 6-hour time point measurement is shown in Figure 7.4 below.

Figure 7.4. *A sample of gel B1 at its 6-hour time point during the non-lyophilised gel swelling experiment. The initially colourless and transparent samples obtained a pink hue as they absorbed the cell culture medium.*

There are various ways to calculate the swelling ratio (SR) of hydrogels. In this case, the swelling ratios were calculated at each time point using formula (4)

$$SR = (W_s - W_d) \,/\, W_d \,, \tag{4}$$

where W_s is the mass of the swollen gel and W_d the mass after freeze-drying. The mass W_d of the lyophilised samples was obtained from time point 0, and the swollen sample mass W_s from the later time points. In the case of the fresh gel samples, W_d was the mass of the gel when removing it from the syringe after one hour of gelation in the incubator. The resulting swelling ratio SR was plotted as a function of time to visualise the swelling kinetics of the gels, as presented later in Chapter 8.5.

7.4.5 *In vitro* enzymatic degradation

Hyaluronic acid is decomposed in the body by the hyaluronidase (HAse) enzymes. Similar degradation was tested *in vitro* for the hydrogels using bovine testicular HAse type I-S (400–1000 U/mg) dissolved in filtered PBS solution. The HAse concentration of the stock solution was 1 mg in 15 ml PBS. For each sample ($V = 100\ \mu l$, $n = 3$) 0.75 ml of HAse solution and 1.25 ml of PBS solution were used, resulting in a final HAse concentration of 20–50 U/mg. A parallel control sample for each gel was made and immersed in 2.0 ml of filtered PBS. The samples were prepared in 1 ml cut syringes and gelated at 37 ºC for 1 hour before immersing them into HAse-PBS solution in 15 ml Falcon® tubes.

The enzymatic degradation was observed by weighing the samples at time points of 0, 2, 4, 6, 24 and 26 hours. Prior to testing, the empty sample tubes were weighed, and at time point 0 the fresh gels were inserted into the empty tubes and the system was weighed. After this, the solutions were added and the gels were weighed at time points of 2, 4, 6, 24 and 26 hours. A sample was concluded to be degraded when no gel was noticeable in the tube when removing the solution.

7.4.6 Effects of air exposure

When implanted in the cornea, the surface of the gels will be exposed to the surrounding air instead of being immersed in a liquid. Being exposed to air might cause possible changes in the dimensions, rigidity, transparency or other properties of the gels, which is why an experimental method was developed for hydrogel air exposure testing as a part of this thesis.

For these experiments, a custom-fabricated apparatus was crafted using a 24-well plate and Millicell® Hanging Cell Culture Inserts with 1 µm pore size (Merck Millipore, Billerica, MA, USA). The cell culture inserts were placed in the wells with their porous bottom in contact with the medium, while the top surface of the gel in the insert is exposed to air. This way the gels, intended to include cells in later experiments, absorb the medium only

through the pores in the base of the insert. To allow the cell culture medium to flow freely between the wells, the bottoms of the wells were cut off and passages were made between the wells and the peripheral edges of the well plate. The apparatus was placed on a petri dish and covered with a lid. During testing, the apparatus was incubated at 37 ºC and the gels were examined at different time points.

Photographs of the apparatus without the gels and the medium are presented in Figure 7.5 below, along with an illustration showing how the gels were situated within the inserts.

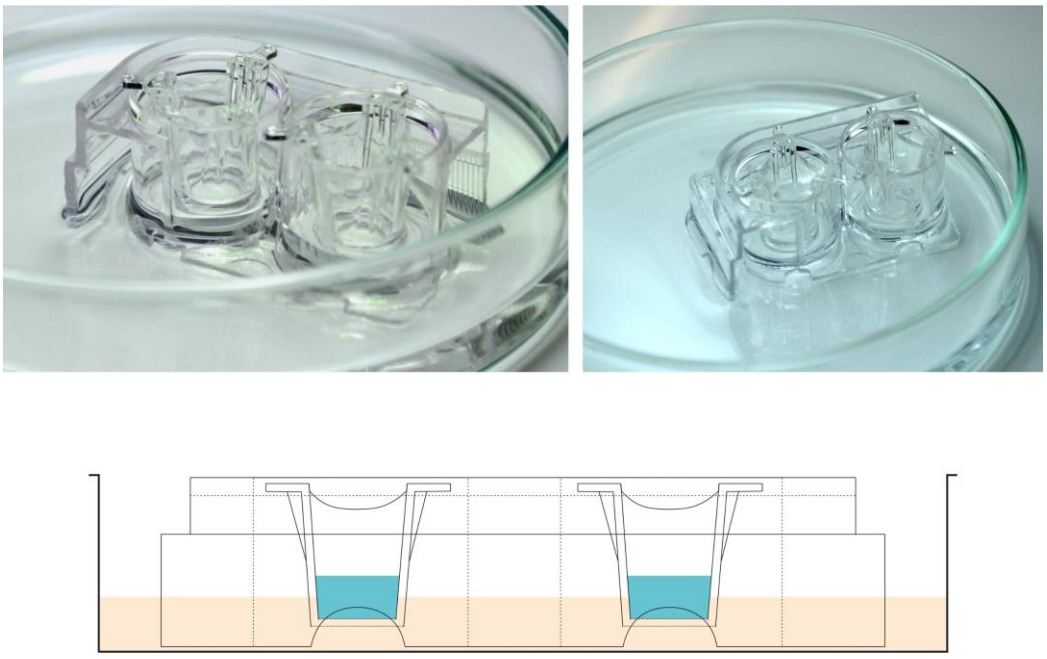

Figure 7.5. *Photographs of the empty system and a cross-sectional illustration of the custom-fabricated apparatus for hydrogel air exposure testing. The gels inside the inserts are presented in blue and the cell culture medium in orange. The whole system was placed in a petri dish and covered to avoid evaporation.*

It was noticed that the elevated temperature caused the medium to evaporate rapidly (within 24 hours), so it was necessary to place the apparatus inside a plastic bag accompanied with an open water container to maintain the humid atmosphere. Alternatively, the system could be placed in the incubator without a plastic bag by placing a large tray of water in the bottom of the incubator.

After a desired time of air exposure, the surface and the edges of the gel were examined visually and with a microscope. To evaluate the possible changes in sample dimensions, such as shrinking, the edges and the surface of the samples were examined with a microscope. To observe gel swelling and changes on the shape of the surface, the gels in the inserts were photographed from the side at different time points.

8. RESULTS

8.1 Gel preparation

A protocol for hyaluronan hydrogel preparation was successfully developed and the optimal compositions for the desired gel types were determined. All the formulations gelated within minutes from component mixing and showed sufficient transparency. From 20 different gel compositions 4 gels were chosen for further material characterisation and will be referred to as presented below:

A1: HA-ALD1 (20) + HA-ADH (10)
A2: HA-ALD1 (22.5) + HA-ADH (11.25) + Rat tail collagen I (2)
B1: HA-ALD2 (30) + HA-CDH (30)
B2: HA-ALD2 (30) + HA-CDH (30) + Rat tail collagen I (2).

8.2 Chemical structure characterisation

Fourier transform infrared spectroscopy (FTIR) was used to investigate the chemical compositions of the polymer components. The FTIR curves of the different gels are presented in Figure 8.1. below.

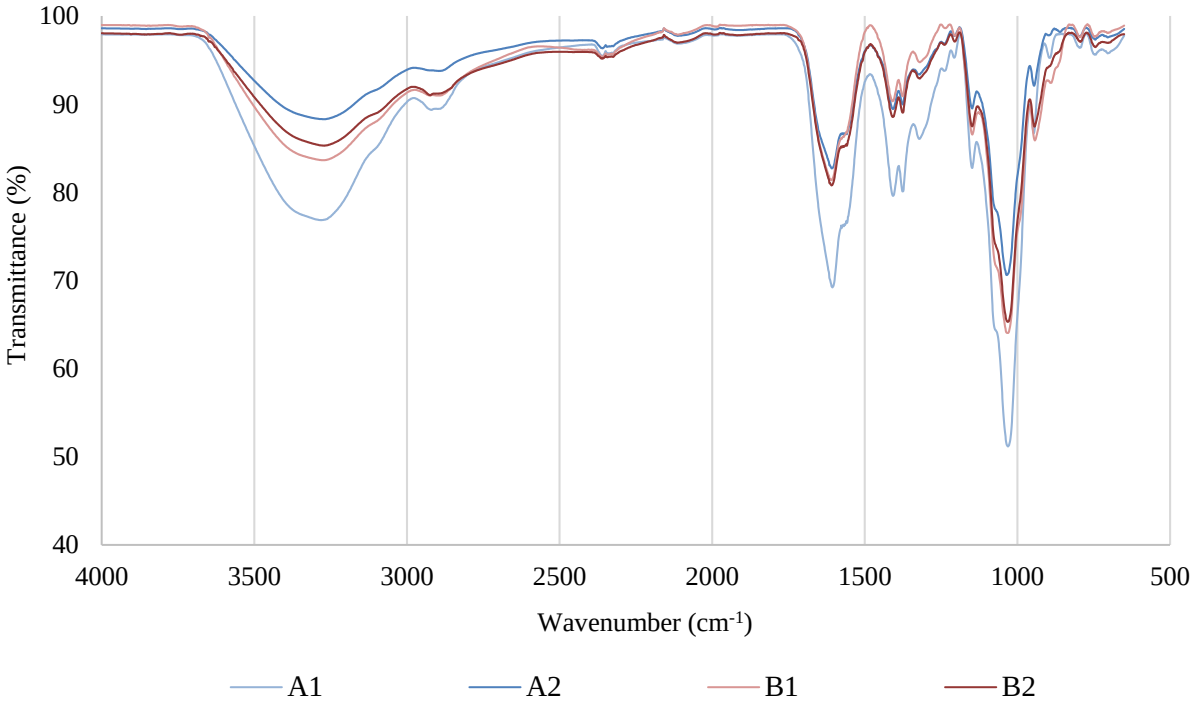

Figure 8.1. *FTIR curves of gels A1, A2, B1 and B2.*

The characteristic signals identified from the FTIR curves for the gels and their components are presented in Table 8.1 below.

Table 8.1. *FTIR signals identified for the characterised hydrogels and their components.*

Component / gel	**Characteristic signals (cm^{-1})**
HA-ALD1	1721 (ν(C=O) of 120 –C(O)H), 1620 (ν(C=O) of –NHC(O)– and C(O)OH)
HA-ALD2	2890 (ν(C-H) of –C(=O)H), 1743 (ν(C=O) of –C(=O)H), 1717 and 1636 (ν(C=O) of amide II), 1621 (δ(N–H) of -NHC(=O)–), 1549 (δ(N–H) of amide II)
HA-ADH	1705 (ν(C=O) of amide II), 1653 (δ(N–H) of amide and amine I), 1562 (δ(N–H) of amine and amide II), 1411 (δ(CH_2–C=O) of –CH_2), 1077 (ν(C–N) of amine)
HA-CDH	1744 (ν(C=O) of amide II), 1648 (ν(C=O) of amide II), 1613 (δ(N–H) of amine I), 1415 (δ(N–H) of amide II), 1073 (ν(C–N) of amine)
Rat tail collagen I	3020 (ν(N–H) of amine II), 1635 (ν(C=O) of amide I), 1550 (δ(N–H) of amide II), 1240 (δ(N–H) of amide III vibration modes), 1080 (ν(C–O–C) and 1033 ν(C–O) of carbohydrate moieties)
HA-ALD1 (20) + HA-ADH (10)	1606 (ν(C=N) of the hydrazone bond)
HA-ALD1 (22.5) + HA-ADH (11.25) + Rat tail collagen I (2)	1605 (ν(C=N) of the hydrazone bond)
HA-ALD2 (30) + HA-CDH (30)	1609 (ν(C=N) of the hydrazone bond)
HA-ALD2 (30) + HA-CDH (30) + Rat tail collagen I (2)	1609 (ν(C=N) of the hydrazone bond)

Symbols: ν = stretching, δ = bending.

In all the hydrogels, the disappearance of the aldehyde signal at 1721 and 1741 cm^{-1} is visible and a new signal from the crosslinking can be recognised at 1605–1609 cm^{-1}, caused by the C=N stretching of the hydrazone bond.

8.3 Mechanical and viscoelastic properties

8.3.1 Mechanical properties

The mechanical characteristics of the hydrogels were determined using unconfined compression testing. From the test data, obtained as the values for load and displacement, the stress-strain curves were calculated for each gel type and further used to calculate the stiffness of different materials. A representative stress-strain graph is presented in Figure 8.2.

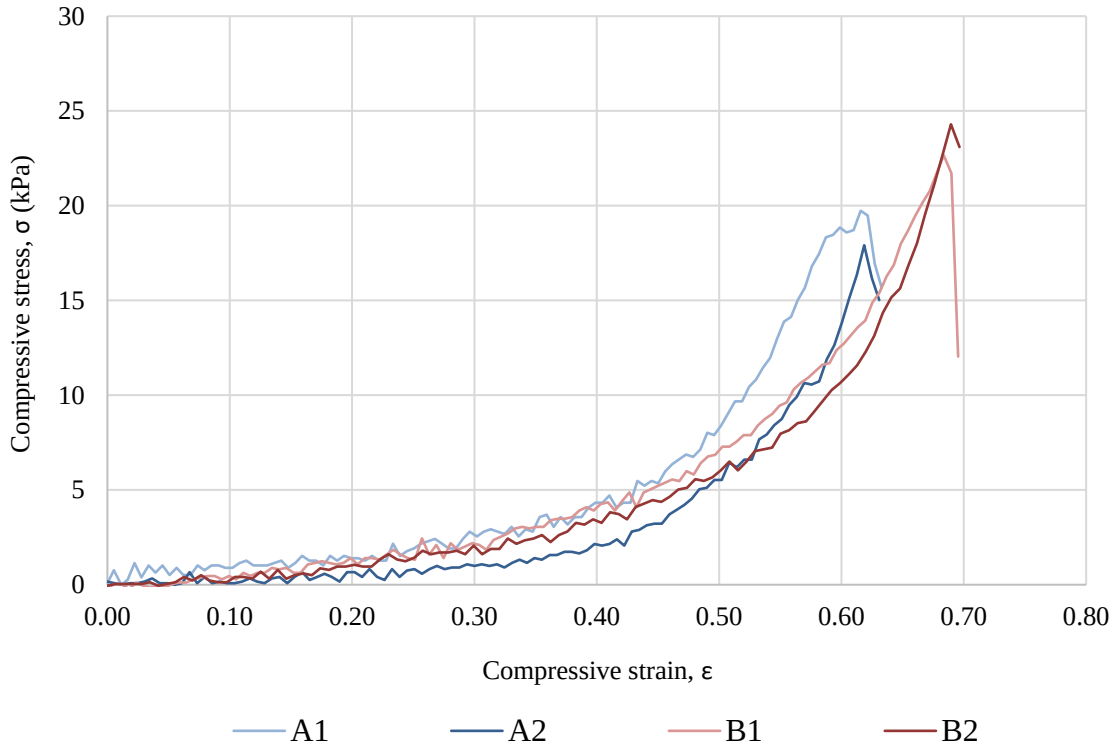

Figure 8.2. *Representative stress-strain curves of the hydrogels from the unconfined compression measurements. For the stiffness calculations and sixth-order polynomial fittings, only values up to the fracture point were used from the stress-strain data.*

Hydrogel stiffness was expressed with the value of their second-order elastic constants, which were calculated from equation (1). The average values for the second-order elastic constants of different gels are collected into following Figure 8.3.

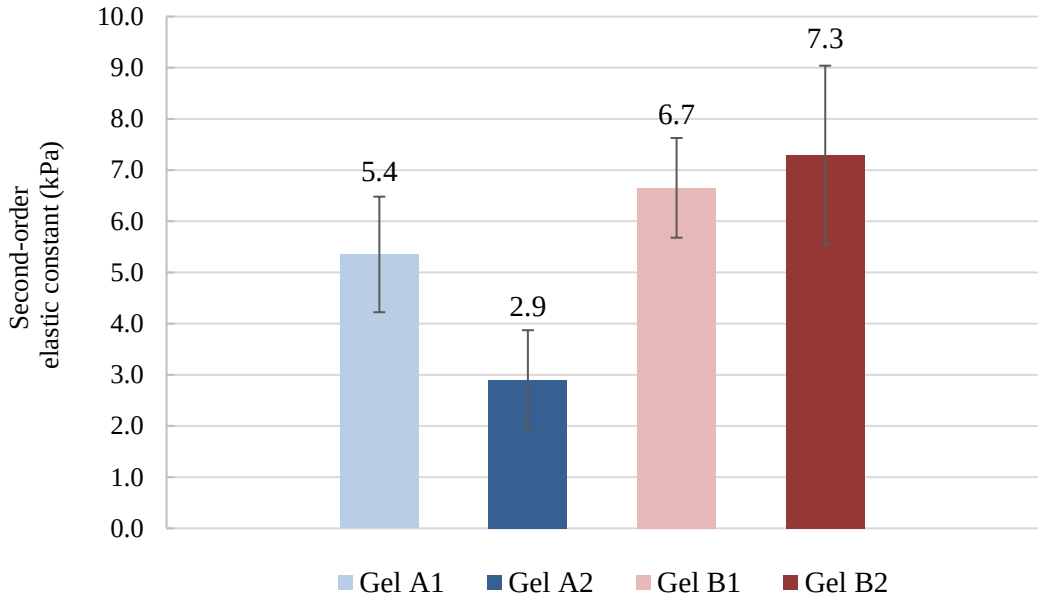

Figure 8.3. *Average (n=5) second-order elastic constants of the different gel types.*

However, for better visualisation and comparison between different strain values, the polynomial functions obtained from equation (2) are presented in relation to strain in Figure 8.4 on the following page.

In the case of the CDH-modified gels, the value of the second-order elastic constant appeared to slightly increase as collagen was added, while the ADH-modified gels with collagen showed a significant decrease. This kind of behaviour was unpredicted, since collagen-content was expected to improve hydrogel stiffness.

Although the second-order elastic constant can be used to describe the mechanical properties of the materials, it does not show how their behaviour changes with different strain values. Moreover, as emphasised in Chapter 7.4.2, these coefficients should be merely considered as estimations, since they were calculated from the average stiffness values at $\varepsilon = 0–0.15$ from the stiffness value with the smallest relative standard deviation. Therefore, it is essential to rather evaluate the hydrogels' mechanical behaviour from their complete stiffness-strain curves, which are presented in Figure 8.4.

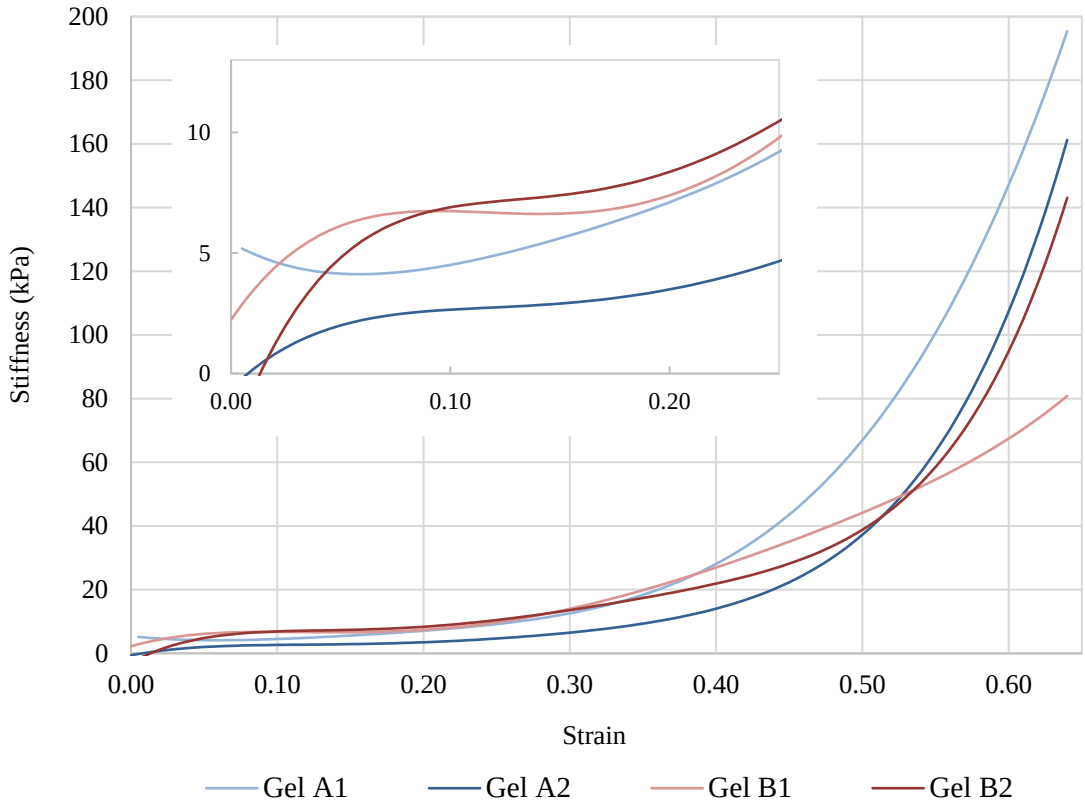

Figure 8.4. *The average (n=5) stiffness-strain curves of the hydrogels. Gel stiffness in the 0–0.25 strain area is zoomed in and presented in the sub-graph.*

As the stiffness-strain curves show, up to about 20 % strain levels the stiffness remains almost constant. After this, it builds up rapidly with the increasing strain value. The value of the second-order elastic constant for each gel was determined below strain values of 0.15 at the average stiffness value with the lowest relative standard deviation.

The type B gels showed superior mechanical properties compared to the type A, as seen in Figure 8.3. The second-order elastic constants of B1 and B2 were (6.7 ± 1.0) kPa and (7.3 ± 1.1) kPa, while the second-order elastic constants of gels A1 and A2 were only (2.9 ± 1.1) and (5.4 ± 1.1) kPa.

8.3.2 Viscoelastic properties

The viscoelastic behaviour of the hydrogels was evaluated in rheological measurements. The linear viscoelastic region (LVR) of the gels was measured through amplitude sweeps, and the values of storage modulus (G') and loss modulus (G'') were determined from the linear region of the frequency sweep curves. These moduli express the way the material can resist shear forces, with G' depicting the elastic and G'' the viscous behaviour.

The amplitude sweep graphs of different gels in Figure 8.5 below show that the LVR is maintained until 0.7–1.0 strain values, after which the storage modulus G' decreases due to the breakdown of the material.

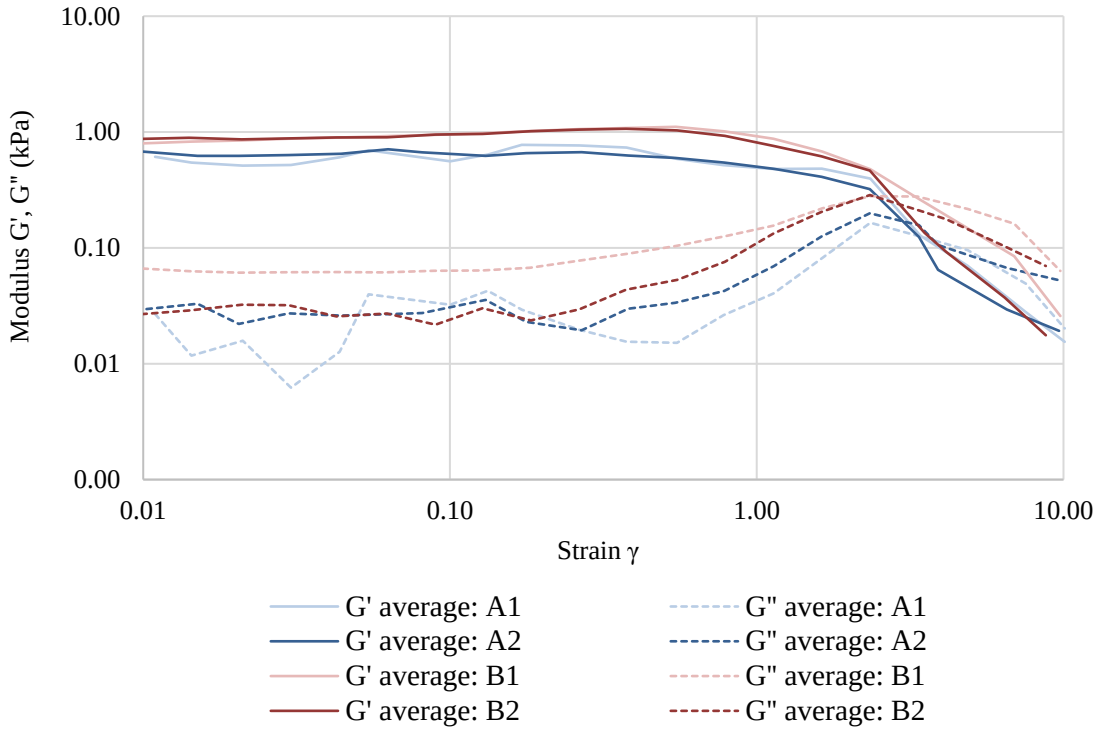

Figure 8.5. *Amplitude sweep measurement: average values (n=2).*

The storage modulus G' and the loss modulus G'' are parallel in the linear viscoelastic region, which is an indication of a true gel structure. For an ideal gel, the storage modulus should have greater values than the loss modulus (G' > G''), which can be observed in the case of the tested gels as well. This signifies that the elastic behaviour of the material dominates its viscous behaviour. The results of the frequency sweep measurements are presented in Figure 8.6.

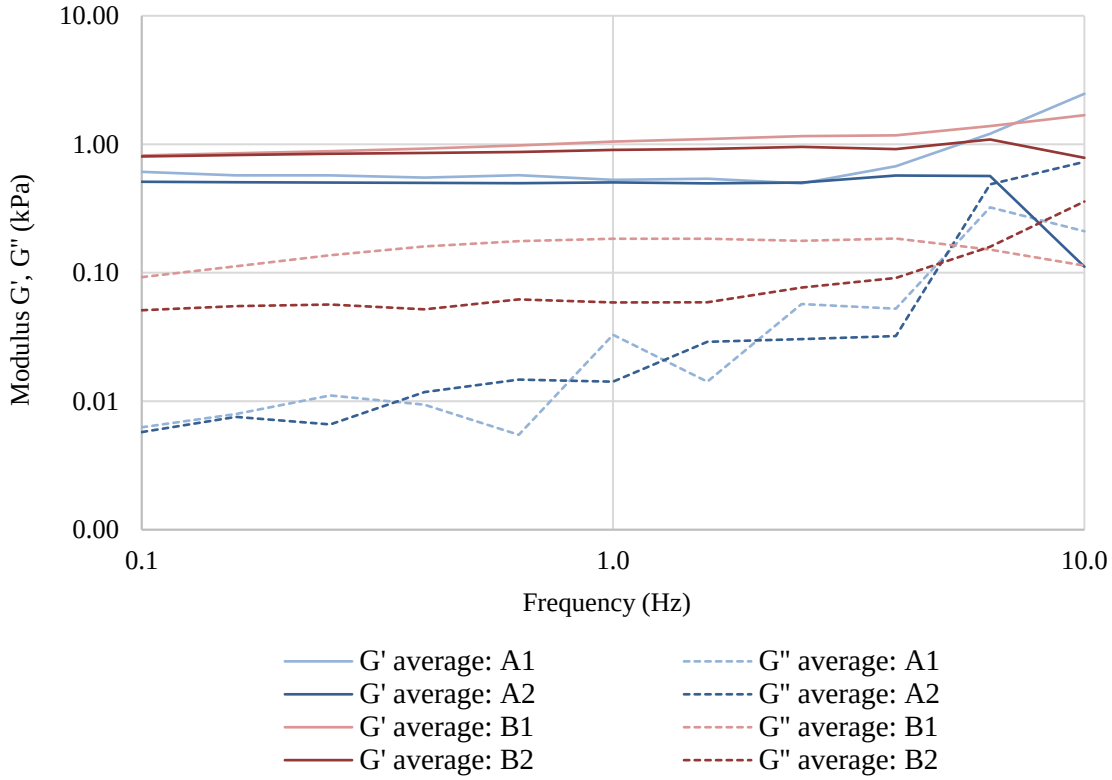

Figure 8.6. *Frequency sweep measurement: average values (n=2).*

Apart from gel B2, the moduli curves presented in the figure correspond to the results of the compression tests. The rheology results indicate that the shear moduli of gel B1 are greater than the ones of B2, while the second-order elastic constant had a higher value for gel B2.

To describe the whole viscoelastic character of the gels, the values of the complex shear modulus G* and *tan δ*, the ratio between the viscous and the elastic modulus, are presented in Table 8.2. The modulus G* combines both the values of the elastic portion G' and the viscous portion G'' to describe the complete viscoelastic behaviour of the material.

Table 8.2. *Average values of the complex modulus G* and tan δ in 0–1.0 Hz frequency range.*

Gel	Average complex modulus G* at 0–1.0 Hz	Average *tan δ* at 0–1.0 Hz
A1	0.57 ± 0.02 kPa	0.022 ± 0.01
A2	0.51 ± 0.03 kPa	0.027 ± 0.01
B1	1.11 ± 0.34 kPa	0.107 ± 0.06
B2	0.81 ± 0.19 kPa	0.082 ± 0.06

The value of *tan δ* is used to evaluate the strength of the gel structure (strong gel: *tan δ* < 0.10, weak gel: *tan δ* > 0.10), as described in Chapter 7.4.2. Table 8.2 shows that gel B1 exceeds this limit. However, because the surpass of *tan δ* value is only minor, the gel was still considered to have a strong gel structure. The greater *tan δ* value might have been caused for example by wetter gel surfaces in the rheology measurement samples, or by uneven mixing of the components.

8.4 Optical properties

8.4.1 Refractive index

The data from the RI measurements was obtained as the values of reflection coefficient and angle of incident, which were used to calculate the refractive indices of different hydrogel samples. The full output graph can be seen in Figure 8.7.

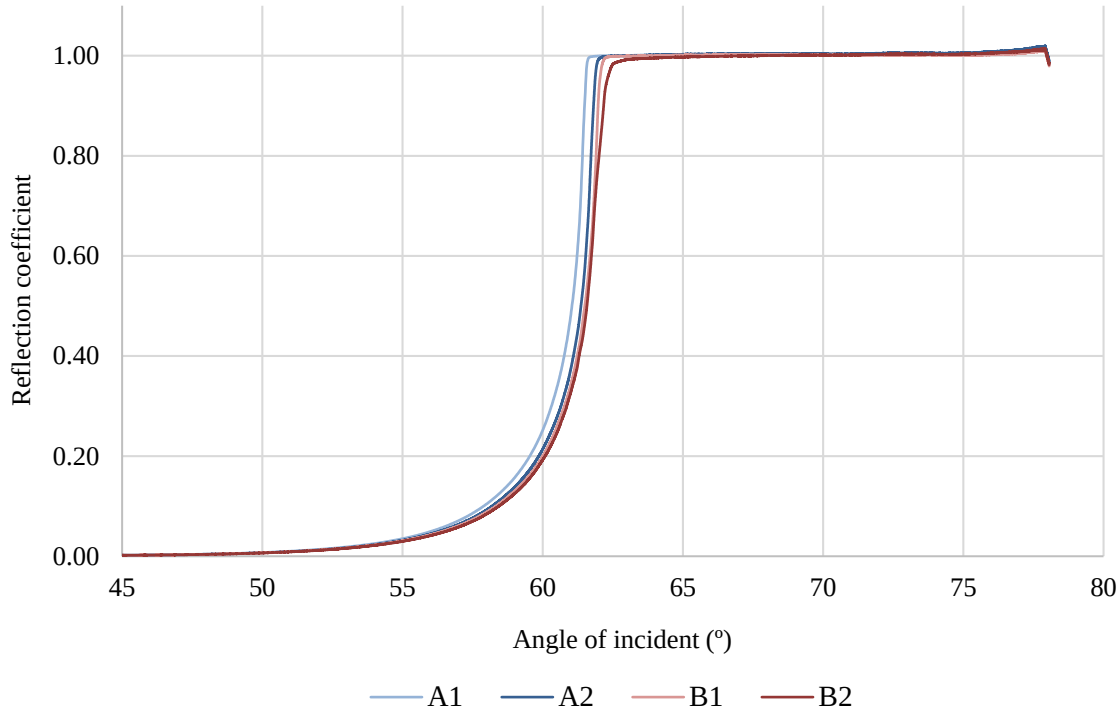

Figure 8.7. *Internal reflection curves of the measured hydrogels from the refractive index measurements.*

However, to determine the angle value that can be used for RI calculation, it was necessary to examine the curve closer. The angle values used in the calculations were taken from the graph by drawing tangent lines on the vertical and horizontal parts of the curve, and determining the angle value at their intersection point. To do this graphical determination with sufficient accuracy, it was necessary to zoom in on the bends of the curves. The essential parts of the reflection coefficient vs. angle of incident-curves are presented in Figure 8.8 below.

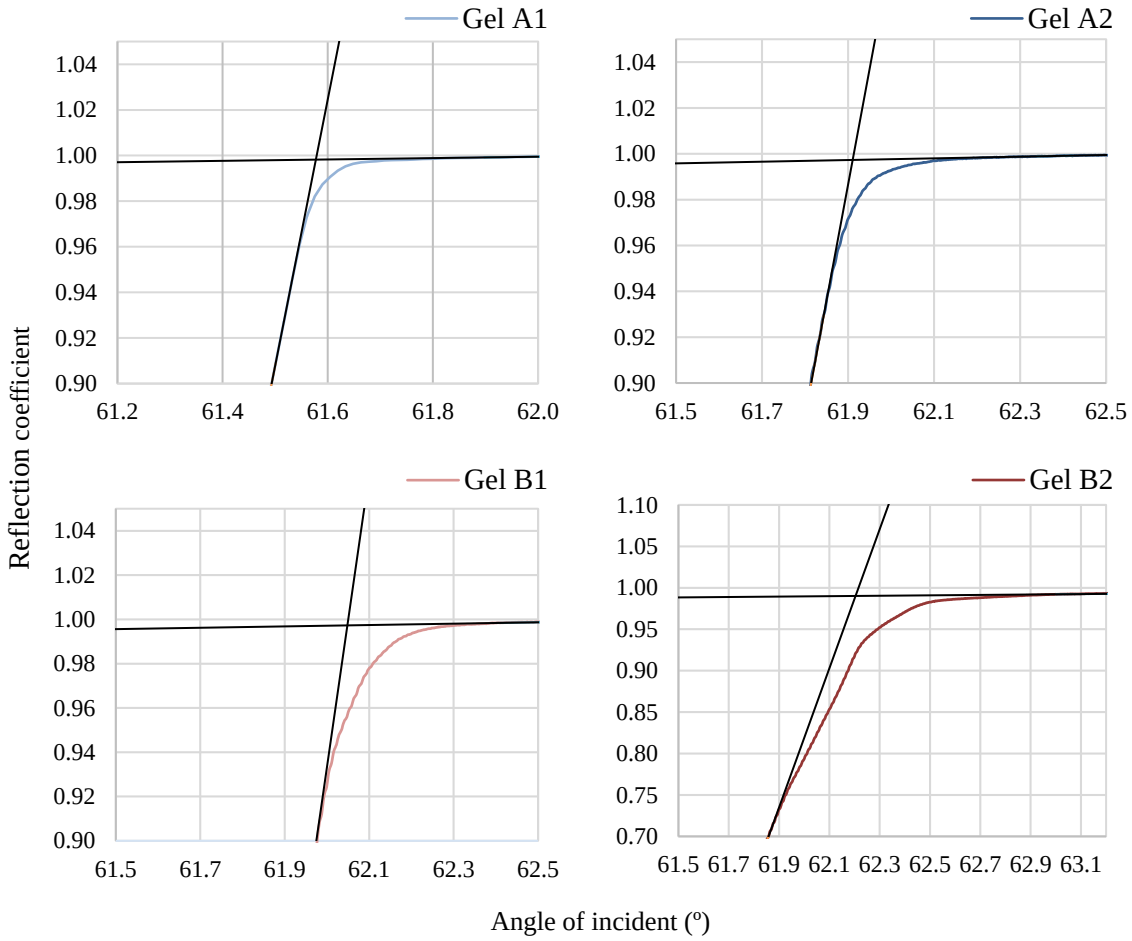

Figure 8.8. *Determination of the angles from the internal reflection curves for the calculation of hydrogel refractive indices. Angle values for gels A1, A2, B1 and B2 from the curves were 61.58, 61.91, 62.05 and 62.21, respectively. Note: A scale adjustment was necessary for gel B2 curve to achieve an appropriate tangent line fitting.*

Figure 8.8 shows that compared to the curves of the other three gels, the curve of B2 is not as consistent at the section where the RI was determined from. To avoid error, it was necessary to zoom out and fit the tangent lines from further parts of the curve.

The angle values for gels were determined visually from the enlarged curves, and the RI values were calculated using the formulae presented in Chapter 6.4.3. The angles of incident, together with the RIs calculated with equation (3), are presented in Table 8.3 on the following page.

It should be noted that this type of graphical method leaves a significant chance for error, which can be caused for example by an inaccurate vertical tangent line. Even a minor change in its direction will cause the angle value to change, which in turn alters the outcome from equation (3).

Table 8.3. *The refractive index of the corneal stroma and the refractive indices of different gels calculated from the RI measurement data.*

Gel	Refractive index	Angle value (º)
A1: HA-ALD1 (20) + HA-ADH (10)	**1.332**	61.58
A2: HA-ALD1 (22.5) + HA-ADH (11.25) + Col (2)	**1.335**	61.91
B1: HA-ALD2 (30) + HA-CDH (30)	**1.337**	62.05
B2: HA-ALD2 (30) + HA-CDH (30) + Col (2)	**1.339**	62.21
Native corneal stroma (Patel et al., 1995)	**1.38**	

The RIs of the hydrogels were slightly greater than the one of water (RI_{water} = 1.33), but still less than of the native corneal stroma, which has an average RI of 1.38 (Patel et al., 1995). Type B gels had slightly higher RIs than the ones of type A, presumably due to their higher crosslink density. The addition of collagen appeared to increase the RI value in both gel types. Overall, however, the differences were minor: only about 0.5 % between the highest (B2) and the lowest (A1) RI values.

Even though type B gels showed higher RI values than the gels of type A, they still do not reach the RI of the natural corneal stroma, which is about 3 % greater. Based on the results, higher content of collagen I contributes to a higher RI, and could therefore improve the refractive power of the hydrogel implant. However, since higher collagen concentrations in the gel optimisation phase resulted in haziness, some improvements would be needed in gel compositions.

8.4.2 Transparency

All the gels were considered sufficiently clear for ophthalmic applications based on visual inspection. As an example, a sample of gel B1 with 10 mm diameter and 1 mm thickness can be seen photographed in Figure 8.9 below.

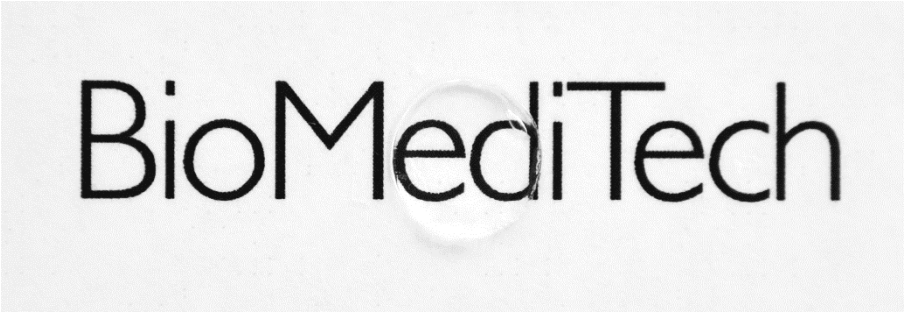

Figure 8.9. *A type B1 hydrogel sample (10 × 1 mm) photographed on top of a printed text to demonstrate gel transparency.*

Gel transparency was examined using a fibre spectrometer, as presented in Chapter 7.4.3. However, there are still major improvements needed for this testing method (see Chapter 9.2), which is why the following results can only be considered suggestive.

The transmittance measurement was conducted for the wavelength range of 300–1000 nm, but with the purpose of evaluating gel transparency for the human eye it is reasonable to only examine the 'visible light' wavelengths of 400–700 nm. The transmittance of UV light would also be a sensible feature to measure for a material targeted for corneal applications, but was considered non-essential at this point of the development.

The measurement was not carried out for all the characterised materials since the method was still incomplete, but an illustrative transmittance curve with gels A1 and A2 and the air reference is shown in Figure 8.10 below.

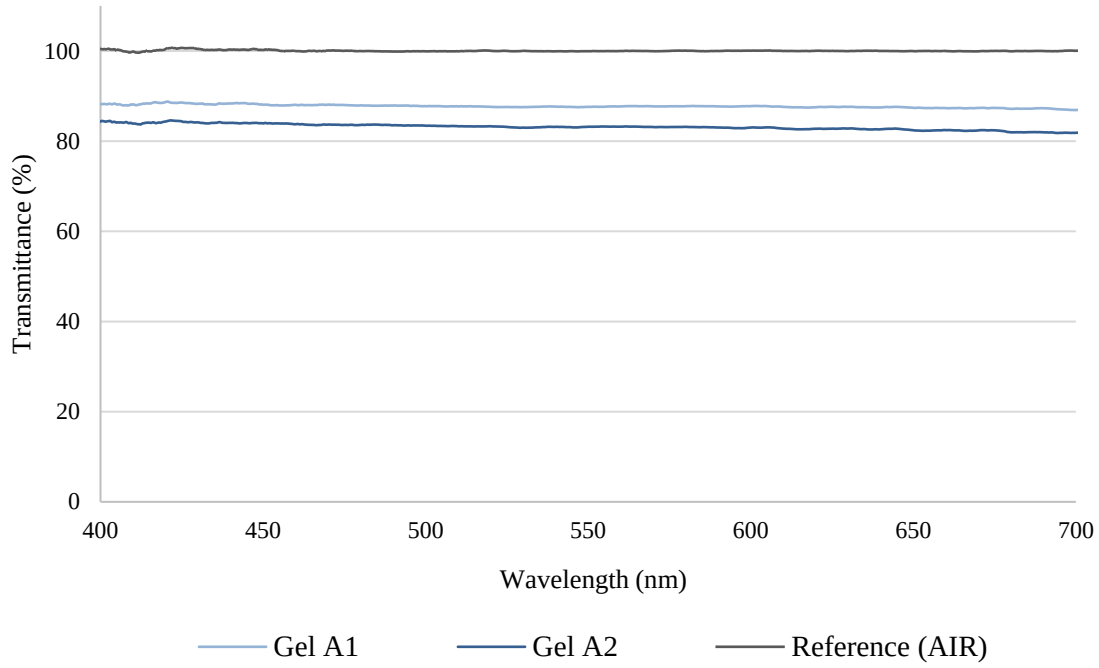

Figure 8.10. *An illustrative figure of a transmittance measurement using a fibre spectrometer and a custom-fabricated hydrogel sample holder.*

Even though the method was lacking reliable repeatability, the results appear reasonable: the air reference used in calibration shows 100 % transmittance, while the collagen-free gel A1 shows superior transparency to its collagenous version, A2. The collagen content in the gels was assumed to increase opacity, which was also observed when optimising the gel compositions. Based on the limited transparency measurements conducted in this study, it can be presupposed that the concentration of collagen is inversely proportional to the transparency of the tested hydrogels. However, since the collagen concentration in the gels was relatively low, no considerable difference is shown in the transmittance levels between the gels A1 and A2.

8.5 Stability and swelling kinetics

The swelling test data was recorded and used for the calculation of mass-based swelling ratio for each gel type. The average SR values of three parallel samples were calculated at different time points and plotted as a function of time up to 48 hours. The test was conducted both for non-lyophilised and lyophilised samples immersed in cell culture medium. The swelling test data for the lyophilised and non-lyophilised gels are presented in Figures 8.11 and 8.12 in respective order.

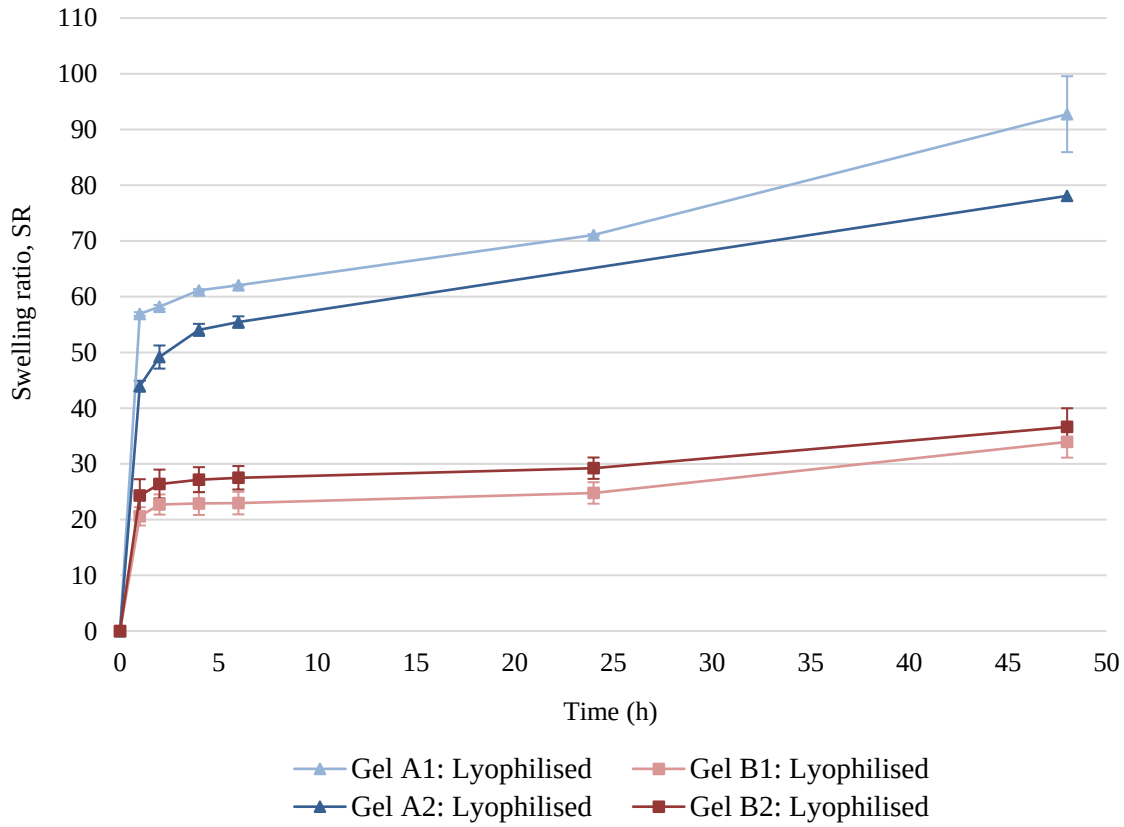

Figure 8.11. *Hydrogel swelling kinetics in the cell culture medium: Average (n=3) swelling ratio curves of the lyophilised samples. Due to a practical issue with the measurements, the 24-hour time point for gel A2 is not included.*

The lyophilised gels showed greater resilience against swelling under the testing conditions and lasted considerably longer than the non-lyophilised samples. The gels of type B maintained their geometrical shape throughout the test, and reached an equilibrium point where they remained until they dissolved through hydrolysis. Type A samples swell more vigorously and kept on absorbing the medium until their structure broke down and the gels broke in pieces.

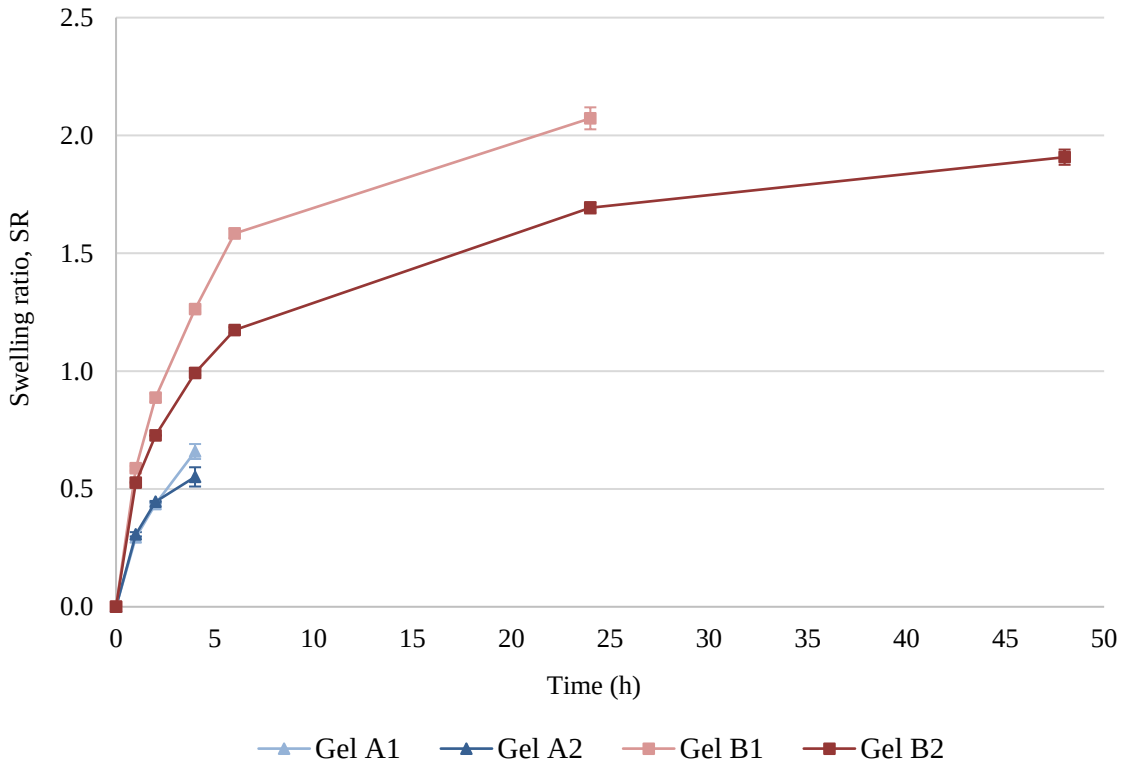

Figure 8.12. *Hydrogel swelling kinetics in the cell culture medium: Average (n=3) swelling ratio curves of the non-lyophilised gel samples.*

The swelling behaviour of the non-lyophilised samples differs considerably from the ones that were lyophilised. Even though the lyophilisation had made the samples more resistant to swelling, they experienced more dimensional deformation as they swell. The non-lyophilised gels dissolved in shorter time, but managed to preserve better their original cylindrical shapes.

As seen from the swelling curves of the lyophilised gels in Figure 8.11, they seemed to reach a sort of ‘equilibrium’ level where the absorption slowed down considerably. By multiplying the average mass of the dry samples by the average SR value of this equilibrium plateau, it is possible to estimate whether the lyophilised samples recovered their original mass or if the freeze-drying process made them unable to return to their initial state. This kind of estimation was done, and it seemed that the lyophilised samples did not return to their original mass. This suggests that the lyophilisation possibly caused physical entanglements, structural collapses or other changes in the polymer network. The collagen content of gels A2 and B2 also decreased the value of the ‘equilibrium’ swelling ratio, when compared to the mass of the corresponding non-lyophilised gels. However, it should be noted that this kind of calculation is mere speculation, and cannot be used as an actual part of the characterisation.

8.6 *In* vitro enzymatic degradation

The enzymatic degradation tests were conducted to ensure that the polymer modification had not affected the hyaluronan molecule in a way that would make it unrecognisable to the hyaluronidase enzymes. Until reaching complete degradation, the 100-µl gel samples ($n = 3$) were immersed in HAse-PBS solution which was changed after weighing at each time point.

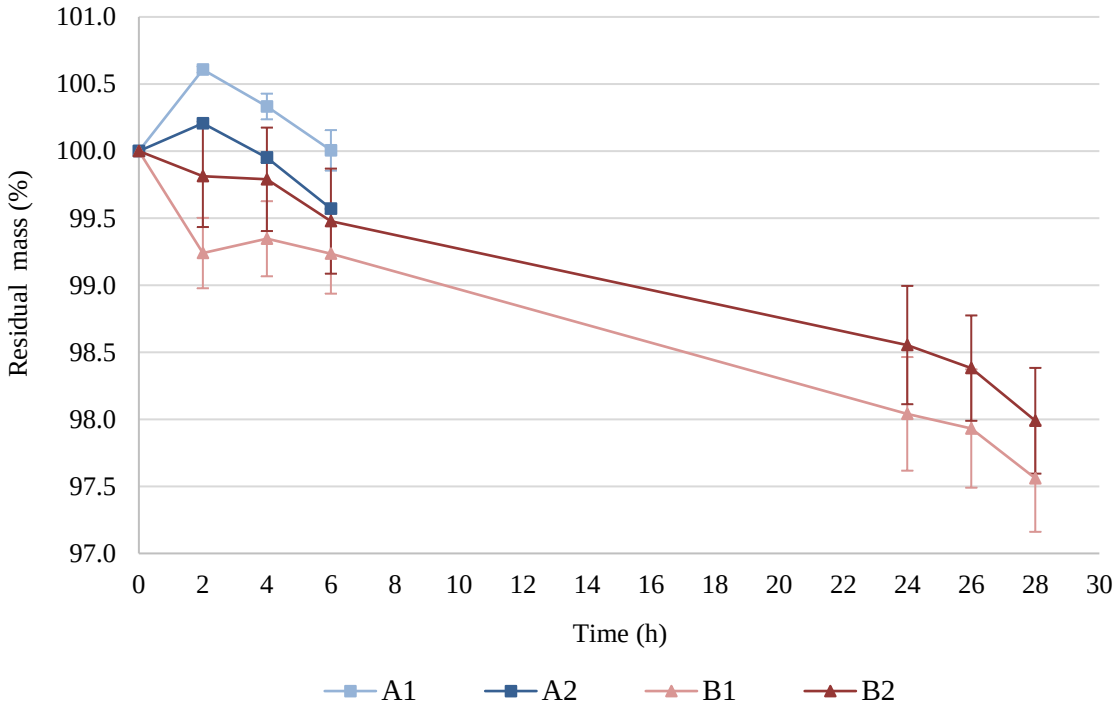

Figure 8.13. *Average (n=3) enzymatic degradation curves of the tested hydrogels. Gels A1 and A2 degraded completely between time points 6 h and 24 h, while gels B1 and B2 degraded between time points 28 h and 48 h.*

The rate of enzymatic degradation of each gel type is presented in Figure 8.13, where their average ($n = 3$) relative masses are plotted as a function of time. In type A gels the degradation was more visible after a period of swelling, which dominated their behaviour up to the 2-hour time point. After this, the gel mass decreased quite rapidly until the gels had been completely degraded by the enzymes between 6 and 24-hour time points. Type B gels resisted considerably better, lasting in the enzyme solution for over 28 hours. At the 48-hour time point, however, all the gels had been degraded by the enzymes.

A slight, unusual decrease is visible at the 2-hour time point of gel B1. The surfaces of the gels had most likely dried more during weighing than at other time points, which resulted in smaller masses. Otherwise the curve of gel B1 closely follows the behaviour

of gel B2. Type B gels also resisted the initial swelling better, and did not show similar mass increase in the first hours like type A gels.

Collagen-content accelerated the rate enzymatic degradation of type A gels, while it slowed down the degradation of gel type B. However, the difference occurs most importantly during the first hours, after which the degradation rates of collagenous and non-collagenous gels seem to continue almost equal with both gel types.

8.7 Air exposure behaviour

The custom-fabricated apparatus performed as expected, allowing the gels to absorb medium through the pores of the inserts. However, due to high absorption the gels tended to swell extensively and dissolve after a certain time. The behaviour was in line with what was observed in the swelling experiments described in Chapter 7.4.4, with a significant difference between the stability of the two gel types A and B.

While all the gels absorbed the medium through the pores in the bottom of the insert and swell, the type A gels did not withstand the swelling for more than 3 days before they dissolved and disappeared from the inserts. Type B gels, on the other hand, kept on absorbing the medium and remained in the inserts as swollen gels throughout the 7-day experiment, as visible in Figure 8.14.

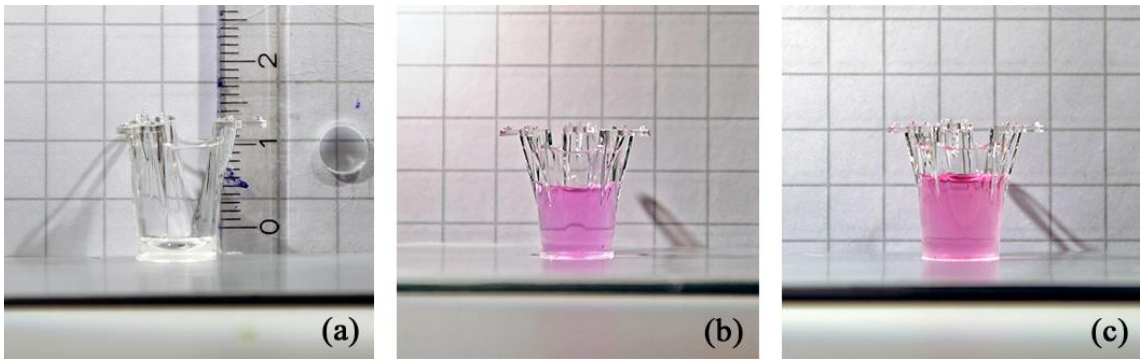

Figure 8.14. *Hydrogel air exposure experiment: Gel B1 after gelation (a), after 3 days (b) and after 7 days (c) in the insert.*

Based on the results, the exposure to atmospheric conditions did not have any significant effect on the gels. The surfaces of the gels were also examined using optical microscopy, but no significant changes, such as drying or deformations, were visible. The dominating behaviour was clearly the absorption of the cell culture medium, which resulted in gel swelling and eventual dissolving caused by the breakdown of its crosslinked polymer network. Like in the swelling tests, gels A1 and A2 did not maintain their structure as well as gels B1 and B2, which lasted in the inserts considerably longer.

9. DISCUSSION

9.1 Evaluation of hydrogel properties for stromal regeneration

In the scope of the characterisation methods carried out in this study, the designed hydrogels showed potential to be used as materials for stromal regeneration. Regarding the mechanical, rheological and optical properties the gels performed sufficiently well. The results from cell culture tests showed satisfactory performance for the hyaluronan hydrogels, whereas the gels containing collagen faced some problems with cell viability, possibly due to too acid pH values.

9.1.1 Mechanical resilience

The main requirements for the mechanical strength of the gels were the adequate rigidity and toughness for the gels to withstand handling during cell culturing and implantation. This requirement was met, since all the gels were sufficiently resilient to be manually handled throughout the characterisations.

The results from the mechanical tests showed a noticeable difference between the gels with different hydrazide modifications, with the CDH-modified hyaluronans of type B showing improved mechanical resilience compared to the type A. However, even though the results of the mechanical tests revealed clear differences between gel types, they were less obvious while handling the gels in practice. All the gels withstood careful handling with tweezers and spatulas during the characterisation, although thin samples, such as the ones in rheology measurements, needed to be handled with special caution. Any sharp edges or shear stress, however, tended to break the gels easily. In the case of the ADH-modified type A gels, increased toughness would be preferable if thin cornea-like slices or films were to be handled. The CDH-modified gels withstood elastic deformation better and could be handled more conveniently.

It should be noted that the calculations for the second-order elastic constants are in fact estimates taken from the 0–0.15 strain range of parallel samples' mean average stiffness values, choosing the value with the lowest relative standard deviation. This strain range includes both the so-called 'toe region' at very low strain values and a part of the non-linear elastic behaviour, which intensifies after 0.15 strain (see Figure 8.4). Therefore, it is more recommended to analyse the mechanical properties of the gels rather by comparing the actual stiffness-strain curves than concentrating too much on the values of the second-order elastic constants.

The gels developed in this thesis can be prepared in physiological or in room temperature by mixing two hyaluronan solutions that crosslink without additional crosslinking agents.

Therefore, they can be applied not only as implants moulded into shapes, but also as injections. In this case, a two-component gel could be used to fix stromal defects by directly injecting it into the corneal tissue from a double syringe. When injected, the mechanical strength of the gels would not have to be as high as if the gel was used as an already-shaped implant, since most of the mechanical stress would obviously be caused during the surgical handling. If used as an injection, however, the resulting hydrogel could be softer, which might have opened new possibilities in the material development and optimisation phase, given it would still be sufficiently strong for corneal cell growth.

A need for an improved gelation platform for the compression test samples was recognised during the characterisation, since some difficulties occurred when removing the samples from the cut 5 ml syringes. As the gels were extruded from the syringes, the peripheral part of their surface tended to 'peel' due to entanglement on the syringe edge. Even though this did not break other than a small part of the gel edges, it could be considered as a minor source of error in the measurements. However, no differences were found in the test data between the intact samples and the ones with 'peeled edges'. It might be possible to solve this problem by using some sort of lubricant on the syringe walls, but adding such agents might also affect the gels. A custom well plate made of polytetrafluoroethylene (PTFE) with openable well-bottoms was tested for this purpose – knowing the material's low coefficient of friction – but the problem persisted. Additionally, the removal of samples from the well plate proved to be problematic compared to the syringes due to the lack of pistons.

9.1.2 Stability, swelling and degradation of the gels *in vitro*

Swelling and stability in cell culture medium

The swelling tests were performed at physiological temperature for freshly gelated and for lyophilised gels by immersing the gels in cell culture medium and observing the changes in their weight as they absorbed water. From the measurements, mass-based swelling ratios were calculated and plotted in relation to time. The tests showed that there were significant differences in the stability of the gels with different hyaluronan modifications.

The CDH-modified gels withstood swelling better before breaking apart, presumably due to the more stable chemical bonds of their crosslinks, as described in Chapter 7.2. The stability of the ADH-modified gels was concluded insufficient, since they dissolved already within the first few hours when immersed in the medium.

Apart from the differences between gel types, the tests showed that the behaviour of the lyophilised gels differed significantly from the ones tested right after gelation. The lyophilised samples maintained their constitution longer in the medium than the non-lyophilised gels, which might result from the forming of physical bonds, such as chain entanglements or structural changes or failures. However, unlike the non-lyophilised samples,

the freeze-dried gels also deformed considerably during swelling, which might also indicate a possible partial collapse of their structure. Interestingly, the lyophilisation also reversed the effect that collagen had on the swelling behaviour of the gels: the lyophilised non-collagenous gels seemed more resistant to swelling, while the fresh gels with collagen showed improved persistence towards the absorption of the medium.

It should be noted that the lyophilised samples do not accurately present the behaviour of the gels that would be used in cell culture experiments, since they are not intended to be dried prior to cell seeding. The results from the swelling tests of non-lyophilised gels can be therefore considered more useful, because they simulate the actual way the gels would be used in practice. However, the measurements for the lyophilised gels were significant as well, since they showed the great impact lyophilisation had on gel swelling and stability. This was also supported by the fact that the gels did not seem to recover their initial mass at the point where the swelling had reached an apparent equilibrium. Even though the reasons for the changes caused by freeze-drying were not clear, the results were relevant regarding for example the possible storage and transportation of the gels.

Enzymatic degradation

The main purpose of the enzymatic degradation test was to ensure that the modifications of hyaluronan had not made it unrecognisable to the hyaluronidase enzymes, which are one of the main factors for implant degradation. All the gels degraded as expected, meaning that the molecule structure had not changed in this aspect. In practice, the gels unrecognised by the enzymes would have remained nondegraded and behaved as they did in the swelling experiments.

The gels of type B withstood hyaluronidase degradation considerably longer than the type A, and experienced rather stable degradation. As time passed, type B samples decreased in size at a stable rate, which visually resembled the mechanism of surface erosion. Type A gels seemed to deform more as they degraded. The difference was not radical, but it might have resulted from the higher crosslink density and improved hydrolytic stability of the CDH-modified gels.

A notable observation is that the masses of all type B samples remained very high throughout the testing, with almost 98 % of their original mass still remaining after 28 hours. This meant a mere 2.0–2.4 percentage point change in mass from time point 0 to 28 hours. After this, all the samples had completely degraded within the next 20 hours, leading to the conclusion that the degradation rate in fact increased towards the end of the experiment. Similar behaviour can be seen in type A gels, with almost 100 % gel mass remaining after 6 hours, and complete degradation occurring before the 24-hour time point. However, because there is rather a long time-gap between time points 6 h and 24 h compared to the data obtained from the time before that (0–6 h), it might not be reliable to draw similar conclusions from gel type A based on this test.

When considering the differences that lyophilisation had on immersed gel behaviour, as discussed in Chapter 8.1.4, it would have been an interesting experiment to include the lyophilised gel samples also in the enzymatic degradation tests. If the HAse enzymes would still recognise the hyaluronan molecules, lyophilisation could be used to improve gel stability by decreasing their swelling rate in the medium. The freeze-drying, of course, might cause problems with how easily the cells and nutrients can move inside the hydrogels during cell culturing. Similar swelling/stability test would could also be carried out with gels that have already corneal cells cultured within to examine what effect the cells have on hydrogel stability and swelling behaviour.

9.1.3 Effects of collagen on mechanical performance and cell viability

Collagen plays a major role as a structural component in the native corneal tissue, which is why it was included as one of the gel component. Due to its ability to form bonds with the aldehyde modified hyaluronan components, collagen was also intended to improve the mechanical resilience of the hydrogels.

As presented in Chapter 8.3.1, the mechanical strength of the collagenous gel B2 (*HA-ALD2 (30) + HA-CDH (30)*) was higher than the one of gel B1 (*HA-ALD2 (30) + HA-CDH (30) + Rat tail collagen I (2)*) without collagen. In contrary, the collagen-containing gel A2 (*HA-ALD1 (22.5) + HA-ADH (11.25) + Rat tail collagen I (2)*) was significantly weaker than the collagen-free gel A1 (*HA-ALD1 (20) + HA-ADH (10)*). The average value of the second-order elastic constant of gel A1 (5.4 ± 1.1 kPa) was over 60 % higher than the one of A2 (2.9 ± 1.1 kPa), while the value of B2 (7.3 ± 1.7 kPa) was about 9 % higher than the one of B1 (6.7 ± 1.0 kPa). Therefore, the addition of collagen improved the mechanical properties in CDH-modified gels, but had a rather radical opposite effect on the ones with ADH-modification. Collagen was suspected to reinforce type B gels by forming additional crosslinks, while distracting the actual crosslinking of HA in type A gels.

The rat tail collagen I used in gels A2 and B2 showed satisfactory cell viability, with both live and dead cells in the suspension on the third day. The collagen-free gels A1 and B1 performed better, with only very few dead cells at the same time point. Another notable feature of the neutralised rat collagen solution was that it did not form a gel on its own when placed in the incubator – opposite to what was expected. Therefore, it is possible that the rat collagen solution had quality problems. However, within the scope of this thesis the reasons for poor collagen performance could not be studied further.

The human collagen solution tested in the optimisation phase caused some undesired outcome in the cell culture tests, which was why its use was discontinued. The human collagen seemed to cause the cells to perish already within three days, with only dead cells

visible in the live/dead analysis. An unsuitable pH value was later concluded as the probable cause, since a test with neutralised pH did not result in as many dead cells. However, like the rat collagen, the human collagen solution did not form a gel on its own, which indicated that there were other problems with the collagen as well. Both the rat and the human collagen were relatively old, which most probably had affected their quality.

9.1.4 Gel biocompatibility

The cell viability tests were carried out at certain points of the optimisation stage to guide the process of material development. All the cell culture tests were conducted by the Eye Group of BioMediTech in Tampere, Finland. The purpose of the tests was to get a first estimation of gel biocompatibility and their suitability in providing a scaffold for corneal cells. The optimal outcome was to observe cell orientation, stretching, functional metabolism and cell stratification throughout the structure of the gel.

As described in Chapter 9.1.3, the collagens caused problems in the cell viability tests. Collagen I from human placenta tested in the optimisation phase turned out to be non-compatible with cells, while the rat tail collagen I showed slightly decreased cell viability compared to the parallel collagen-free gels. Therefore, based on this study the gels without collagen would be better suitable to be used for corneal regeneration. However, since it is possible that the quality of the collagen solutions affected the results, more tests should be done with newer collagen batches.

Generally, the final gels showed sufficient properties to maintain cell growth, but did not induce the cells to orientate or to stretch along the collagen fibres, as was anticipated. Live cells remained on multiple levels of the gel, but tended to remain round-shaped and stationary. During time, more cells gathered on the bottom of the cultures, which indicated that the cells possibly did not to find convenient anchoring points in the gel structure. Although the gels on their own did not principally promote cell growth, it could perhaps be induced with the addition of growth factors or other agents.

The ADH-modified gels A1 and A2 provided weaker mechanical support for the cells than gels B1 and B2 with the stronger CDH-modified hydrazide component. During cell culturing the ADH-modified gels tended to weaken and dissolve prematurely, which is why the CDH-modified gels were a preferable option from this aspect too. In cell viability, no significant differences were noticed between the gel types A and B.

Nevertheless, none of the characterised gels exhibited cytotoxicity or other radical adverse effects on cell growth, which was the essential requirement and the property examined in these tests. Based on the results, the hyaluronan hydrogels A1 and B1 could become satisfactory scaffolds for tissue growth, while the gels A2 and B2 would still need improvements regarding the collagens.

9.2 Characterisation of the optical properties of hydrogels

The optical clarity of the gels was evaluated visually during the optimisation phase as well as during different characterisations. Based on visual inspection, the tested gels showed sufficient transparency to be used for corneal implantation. As the gel clarity was evaluated and different methods were searched from literature, it was noticed that currently no standardised scientific testing protocol has been established for hydrogel transparency measurements. Current methods often involve visual inspection, which is highly subjective and impossible to compare between different research groups. Images of gels with text in the background, which are often used, can merely show that the gels are not completely opaque, and can easily be modified through image editing programs. To produce more objective results and numeric data, a fibre spectrometer-based transmittance measurement method was developed along the characterisations.

Some objective measurement methods have been described in literature to evaluate hydrogel transparency. These include for example ultraviolet-visible (UV-vis) spectroscopy and photography-based optical measurements and calculations (for example Gonzales-Andrades *et al.*, 2015). As described in Chapter 7.4.3, a portable spectrometer with fibre optics and a computer program to evaluate gel transmittance levels was used in this study. Preliminary results were obtained, and they were in accordance to the expectations. Transmittance data showed a difference between gels A1 and A2, confirming that collagen-content actually decreased gel transparency, even though any difference could not be seen with the naked eye. However, further development is still necessary for the sample holder to ensure that both microscopy slides are completely parallel to the penetrating light beam.

The system was first developed with only one microscopy glass and a PDMS membrane. However, when preparing the gels in the PDMS wells it was noticed that due to the capillary effect the hydrogels tended either to form convex lens-like shapes, with the centre being thicker than the periphery, or to ‘climb’ onto the walls of the PDMS well and forming a concave surface. In both cases, it was impossible to maintain control of the gel thickness, which would be essential for the repetition of this type of optical measurement. The solution was to place a second microscopy glass and the metal spacers. By preparing the gel samples so that they remain in the convex shape, with their centre slightly thicker than the PDMS membrane, it was possible to squeeze the gels between the two glasses and achieve a uniform gel thickness. The metal spacers kept the distance between the glasses equal on both sides and were to keep them parallel.

Even though the glasses were highly parallel, the light beam presumably reflected between the glasses and caused error in the results. To avoid light reflection between the slides, distilled water could be used instead or air as the reference. Water as a reference would have possibly decreased light reflection by lowering the differences in RI at the glass-intermediate interface. This idea, however, was not tested in practice due to the lack

of PDMS membrane with appropriate thickness. The membrane used in the measurements was slightly thinner than the metal spacers, which worked well for the hydrogels but would have left a gap for the water to leak out from the PDMS well. Another improvement point would be a proper mount for the sample holder, which would keep it parallel to the light beam and attached to the spectrometer. The mount could be manufactured for instance through 3D-printing, but due to the lack of time it could not be developed during this thesis. Additionally, to avoid error caused by stray light, a removable cover could be added on the mount.

It was not concluded if finishing this custom design would guarantee reliable results, even though the idea seemed to function. An alternative option for fibre spectrometer measurements would be the use of microliter-sized cuvettes. Since the fibre spectrometer was already equipped with a holder for a standard cuvette of 10 mm path length, it could be possible to do the measurements by using, for example, a 500 µl-volume microcuvette that would fit in the standard holder. However, the requirement for such cuvette would be a thin geometry for the sample compartment so that the measurement could be taken from a gel with similar thickness to the native cornea. In many microcuvettes, the sample chamber is thin, but the measurement is made in the longitudinal direction, which would not solve the problem. Therefore, the cuvette would need to be one with a possibility to measure in the transverse (thin sample) direction, having a clear window on all sides of the sample chamber. Compared to the custom apparatus, this method would have the advantage of being relatively free from sources of human error and being easily repeatable in other research groups as well. Unfortunately, there was no possibility to perform tests using this method during this thesis project.

9.3 Transparency vs. biodegradability in tissue-engineered corneal substitutes

Compared to other characterisation methods, it seems that the transparency of hydrogels remains a slightly problematic property to measure. In the stage of material development of this thesis, transparency was also noticed to be a major limitation that prohibited the use of wide range of materials and designs, such as composite structures or higher concentrations of certain components.

However, when considering the actual end use of the gel as a tissue engineered implant for corneal regeneration, it should be noted that even if the material was fully transparent at the moment of implantation, the postsurgical healing process would nevertheless require the eye to be covered for a certain time period. This awoke discussion about how important initial transparency actually is for a biodegradable ocular implant that is designed to be replaced with ocular tissue in a relatively short period of time. In other words, what is the relationship between normal eyesight recovery time after an ocular surgery and the degradation time of a tissue-engineered hydrogel implant; is it possible to design

the implant to degrade during the limits of normal post-surgical recovery time of the eyesight?

Relevant points of comparison for eyesight recovery times are traditional methods of keratoplasty, the most common treatments for severe corneal traumas. These include full thickness corneal grafts, implanted using PK or through DALK, in which Descemet's membrane and endothelium are left intact. However, because the *in vivo* degradation times of the materials developed in this study are not known due to the early stage of development, it is only possible to evaluate results found about similar materials from literature.

In a review of 100 cases of PK done by Sutton *et al.* (2008), two months after the operation about 2/3 of the patients had recovered a best corrected visual acuity (BCVA) value of 6/12, which is half of the value of a healthy eye, while all the patients reached the value after 6 months. The average time to reach a the BCVA of 6/12 was 9,6 weeks. (Sutton et al., 2008) While the results presented in the review are very positive, it has also been reported (Anshu et al., 2012) that the recovery to a similar visual acuity level after a PK might take even 2 to 8 years. The outcome of is highly dependent on the individual and their history in corneal diseases. Generally, the eyes treated with PK often require a long follow-up period and have a relatively high graft failure rate of about 10 %. Over time, however, the successful cases of PK can often result in completely recovered BCVA of 6/6. (Anshu et al., 2012)

Based on the review by Sutton *et al.* it seems that the recovery of a functional level of eyesight after a PK takes at least two months. Hypothetically, if a tissue-engineered corneal implant would begin to integrate into the corneal tissue during this time, there would be no need for the material to be transparent in the first place. The goal would be to observe increasing corneal clarity as the biomaterial degrades and integrates into the tissue, and finally becoming completely clear and healed cornea. Basically, since the operation of implanting a foreign material into the corneal tissue would be alike the one of keratoplasty, the nature of the recovery process would possibly be similar as well. However, as the hydrogel implant is intended to contain cells seeded from the patient's own eye, the biocompatibility of the material might be superior to a corneal transplant.

The biodegradation time of a hydrogel for corneal regeneration depends on the polymer. For the hydrogels prepared in the experimental part of this thesis, the degradation is designed to occur through hydrolysis and enzymatic degradation by corneal hyaluronidase and collagenase enzymes. Even though similar HA-HA hydrogels have not been tested *in vivo*, pre-clinical testing data is available from hydrogels prepared from other natural polymers such as collagen (Liu et al., 2008), chitosan and alginate (Liang et al., 2011). Even though the materials are not completely comparable, these studies with natural proteins could give some reference to predict how the hydrogels in this study would behave *in vivo*.

In their research, Liu *et al.* (2008) prepared a corneal substitute from recombinant human collagen and tested it in pig models through DALK. They reported minor haziness in the implants during the first weeks after implantation, but after 3 months the implants had become fully transparent. In this case, the implant was prepared from collagen, so instead of rapid degradation of the material the purpose was full integration of the implant into the host tissue, which Liu *et al.* observed 1 year after implantation. (Liu et al., 2008) Since collagen is the main structural component of the cornea, good tissue response could be expected.

10. CONCLUSIONS

In this thesis, two types of hyaluronan-based hydrazone-crosslinked hydrogels were studied with and without the incorporation of collagen I. The hydrogel properties were characterised using a wide variety of test methods, and their suitability to be used as materials for corneal regeneration was evaluated.

The mechanical and viscoelastic properties of the hydrogels were examined using compression testing and cone-and-plate rheometry. The refractive indices and optical clarity were determined with customized testing protocols using SPR equipment and a fibre spectrometer. The synthesized polymers were structurally characterised through FTIR spectroscopy. Stability and behaviour under physiological conditions was evaluated at 37 ^{o}C through swelling (DMEM) and enzymatic degradation tests (PBS). To assess hydrogel suitability for corneal implantation and to determine the requirements for further material development, cell viability tests were carried out by a collaborating research group.

The hyaluronans were modified with aldehyde and hydrazide functionalities to enable them to form a three-dimensional gel networks in mild conditions through hydrazone crosslinking. Four hydrogels were chosen for the characterisations. The two components of type A gels were modified with an adipic acid dihydrazide (HA-ADH) reactive group and with a corresponding aldehyde-modified component (HA-ALD1). The components of type B gels were modified with a carbodihydrazide (HA-CDH) reactive group and with a complementary aldehyde-modified hyaluronan (HA-ALD2). Each of the two hydrazone-crosslinked gel types had a gel incorporated with rat tail collagen I and one without.

Type B gels showed potential to be used as a scaffold for cell delivery, or as an *in situ*-crosslinkable hydrogel to fix corneal tissue. The CDH-modified type B gels showed superior mechanical properties compared to type A gels with the ADH modification, as well as better stability and controlled swelling in physiological conditions. The ADH-modified gels did not remain stable in the cell culture medium for longer than three days, which was considered insufficient. All the tested gels were recognised by the hyaluronidase enzymes, indicating that the material can degrade in the ocular tissue through natural mechanisms. Unexpectedly, the addition of collagen I weakened the mechanical properties in type A gels, but had the opposite effect on type B gels. The addition of collagen also increased the swelling of lyophilised type B gels, while decreasing the swelling of type A samples. Collagen content had the opposite effect on the non-lyophilised samples. However, any definite explanation for these results was not confirmed.

Based on this study, the CDH-modified type B gels can be concluded to present the sufficient biocompatibility, stability and mechanical and optical properties to be considered as a potential material for corneal regeneration.

REFERENCES

Ahmad, S. (2012). Concise review: Limbal stem cell deficiency, dysfunction, and distress. Stem Cells Translational Medicine, Vol. 1(2), pp. 110-115.

Al-Yousuf, N., Mavrikakis, I., Mavrikakis, E. & Daya, S.M. (2004). Penetrating keratoplasty: indications over a 10-year period. The British journal of ophthalmology, Vol. 88(8), pp. 998-1001.

ASTM Standard F2900. (2011). Standard Guide for Characterization of Hydrogels used in Regenerative Medicine. ASTM International, West Conshohocken, PA, USA.

Borene, M.L., Barocas, V.H. & Hubel, A. (2004). Mechanical and cellular changes during compaction of a collagen-sponge-based corneal stromal equivalent. Annals of Biomedical Engineering, Vol. 32(2), pp. 274-283.

Burdick, J.A. & Prestwich, G.D. (2011). Hyaluronic Acid Hydrogels for Biomedical Applications. Advanced Materials, Vol. 23(12), pp. H41-H56.

Carlsson, D.J., Li, F., Shimmura, S. & Griffith, M. (2003). Bioengineered corneas: how close are we? Current opinion in ophthalmology, Vol. 14(4), pp. 192-197.

Chen, J., Li, Q., Xu, J., Huang, Y., Ding, Y., Deng, H., Zhao, S. & Chen, R. (2005). Study on biocompatibility of complexes of collagen-chitosan-sodium hyaluronate and cornea. Artificial Organs, Vol. 29(2), pp. 104-113.

DelMonte, D.W. & Kim, T. (2011). Anatomy and physiology of the cornea. Journal of Cataract and Refractive Surgery 37, 3, pp. 588-598.

Duncker, G.I.W., Storsberg, J. & Müller-Lierheim, W.G.K. (2014). The fully synthetic, bio-coated MIRO® CORNEA UR keratoprosthesis: development, preclinical testing, and first clinical results. Spektrum der Augenheilkunde, Vol. 28(6), pp. 250-260.

Dupps, W.J. & Wilson, S.E. (2006). Biomechanics and Wound Healing in the Cornea. Experimental eye research, Vol. 83(4), pp. 709-720.

Fagerholm, P., Lagali, N.S., Carlsson, D.J., Merrett, K. & Griffith, M. (2009). Corneal Regeneration Following Implantation of a Biomimetic Tissue-Engineered Substitute. Clinical and Translational Science, Vol. 2(2), pp. 162-164.

Freegard, T.J. (1997). The physical basis of transparency of the normal cornea. Eye (London, England), Vol. 11 (Pt 4), pp. 465-471.

Ghezzi, C.E., Rnjak-Kovacina, J. & Kaplan, D.L. (2015). Corneal tissue engineering: recent advances and future perspectives. Tissue engineering, Part B, Reviews, Vol. 21(3), pp. 278-287.

Gold, M.H. (2007). Use of hyaluronic acid fillers for the treatment of the aging face. Clinical Interventions in Aging 2, 3, pp. 369-376.

Hassell, J.R. & Birk, D.E. (2010). The molecular basis of corneal transparency. Experimental eye research, Vol. 91(3), pp. 326-335.

Hazra, S., Nandi, S., Naskar, D., Guha, R., Chowdhury, S., Pradhan, N., Kundu, S.C. & Konar, A. (2016). Non-mulberry Silk Fibroin Biomaterial for Corneal Regeneration. Scientific Reports, Vol. 6, pp. 21840.

Hein, C.D., Liu, X.M. & Wang, D. (2008). Click Chemistry, a Powerful Tool for Pharmaceutical Sciences. Pharmaceutical research, Vol. 25(10), pp. 2216-2230.

Hennink, W.E. & van Nostrum, C.F. (2002). Novel crosslinking methods to design hydrogels. Advanced Drug Delivery Reviews, Vol. 54(1), pp. 13-36.

Hopkinson, A., McIntosh, R.S., Tighe, P.J., James, D.K. & Dua, H.S. (2006). Amniotic membrane for ocular surface reconstruction: donor variations and the effect of handling on TGF-beta content. Investigative ophthalmology & visual science, Vol. 47(10), pp. 4316-4322.

Ihanamäki, T., Pelliniemi, L.J. & Vuorio, E. (2004). Collagens and collagen-related matrix components in the human and mouse eye. Progress in retinal and eye research, Vol. 23(4), pp. 403-434.

Islam, M.M., Ravichandran, R., Olsen, D., Ljunggren, M.K., Fagerholm, P., Lee, C.J., Griffith, M. & Phopase, J. (2016). Self-assembled collagen-like-peptide implants as alternatives to human donor corneal transplantation. RSC Advances, Vol. 6(61), pp. 55745-55749.

Jakus, M.A. (1956). Studies on the cornea. II. The fine structure of Descemet's membrane. The Journal of Biophysical and Biochemical Cytology, Vol. 2(4), pp. 243-252.

Karvinen, J., Koivisto, J.T., Jönkkäri, I. & Kellomaki, M. (2017). The production of injectable hydrazone crosslinked gellan gum-hyaluronan-hydrogels with tunable mechanical and physical properties, Journal of the mechanical behavior of biomedical materials, Vol. 71pp. 383-391.

Kolb, H.C., Finn, M.G. & Sharpless, K.B. (2001). Click Chemistry: Diverse Chemical Function from a Few Good Reactions. Angewandte Chemie (International ed.in English), Vol. 40(11), pp. 2004-2021.

Kontturi, L. (2014). Cell encapsulation in hydrogels for long-term protein delivery and tissue engineering applications. University of Helsinki, Faculty of Pharmacy, Centre for drug research, Division of pharmaceutical biosciences, Doctoral dissertation, 124 p.

Kruse, F.E., Rohrschneider, K. & Völcker, H.E. (1999). Multilayer amniotic membrane transplantation for reconstruction of deep corneal ulcers. Ophthalmology, Vol. 106(8), pp. 1504-1511.

Lawrence, B.D., Marchant, J.K., Pindrus, M.A., Omenetto, F.G. & Kaplan, D.L. (2009). Silk film biomaterials for cornea tissue engineering. Biomaterials, Vol. 30(7), pp. 1299-1308.

Liang, Y., Liu, W., Han, B., Yang, C., Ma, Q., Song, F. & Bi, Q. (2011). An *in situ* formed biodegradable hydrogel for reconstruction of the corneal endothelium. Colloids and Surfaces B: Biointerfaces, Vol. 82(1), pp. 1-7.

Liang, Y., Liu, W., Han, B., Yang, C., Ma, Q., Zhao, W., Rong, M. & Li, H. (2011). Fabrication and characters of a corneal endothelial cells scaffold based on chitosan. Journal of materials science, Materials in medicine, Vol. 22(1), pp. 175-183.

Liu, J., Lawrence, B.D., Liu, A., Schwab, I.R., Oliveira, L.A. & Rosenblatt, M.I. (2012). Silk Fibroin as a Biomaterial Substrate for Corneal Epithelial Cell Sheet Generation. Investigative ophthalmology & visual science, Vol. 53(7), pp. 4130-4138.

Lynn, A.K., Yannas, I.V. & Bonfield, W. (2004). Antigenicity and immunogenicity of collagen. Journal of biomedical materials research, Part B, Applied biomaterials, Vol. 71(2), pp. 343-354.

Malvern Instruments. (2015). Evaluating the rheological properties of hyaluronic acid hydrogels for dermal filler applications. Malvern Instruments, web page. Available (accessed 15.08.2016): http://www.malvern.com/en/support/resource-center/application-notes/AN150112-prop-HA-hydrogels-Dermal-Filler.aspx.

Martínez-Sanz, E., Ossipov, D.A., Hilborn, J., Larsson, S., Jonsson, K.B. & Varghese, O.P. (2011). Bone reservoir: Injectable hyaluronic acid hydrogel for minimal invasive bone augmentation. Journal of Controlled Release Vol. 152(2), pp. 232-240.

Meek, K.M. (2009). Corneal collagen – its role in maintaining corneal shape and transparency. Biophysical Reviews Vol. 1(2), pp. 83-93.

Michelacci, Y.M. (2003). Collagens and proteoglycans of the corneal extracellular matrix. Brazilian journal of medical and biological research = Revista brasileira de pesquisas medicas e biologicas, Vol. 36(8), pp. 1037-1046.

Nakajima, H. (2015). APPENDIX B: Table of Refractive Indices for BK7, in: Optical Design Using Excel: Practical Calculations for Laser Optical Systems. 1st ed., John Wiley & Sons Singapore Pte Ltd, pp. 277-278.

O'Leary, L.E., Fallas, J.A., Bakota, E.L., Kang, M.K. & Hartgerink, J.D. (2011). Multi-hierarchical self-assembly of a collagen mimetic peptide from triple helix to nanofibre and hydrogel. Nature chemistry, Vol. 3(10), pp. 821-828.

Oommen, O.P., Wang, S., Kisiel, M., Sloff, M., Hilborn, J. & Varghese, O.P. (2013). Smart Design of Stable Extracellular Matrix Mimetic Hydrogel: Synthesis, Characterization, and In Vitro and In Vivo Evaluation for Tissue Engineering. Advanced Functional Materials, Vol. 23(10), pp. 1273-1280.

Ossipov, D.A., Piskounova, S., Varghese, O.P. & Hilborn, J. (2010). Functionalization of Hyaluronic Acid with Chemoselective Groups via a Disulfide-Based Protection Strategy for In Situ Formation of Mechanically Stable Hydrogels. Biomacromolecules Vol. 11(9), pp. 2247-2254.

Patel, S., Marshall, J. & Fitzke, F.W. (1995). Refractive index of the human corneal epithelium and stroma. Journal of refractive surgery, Vol. 11(2), pp. 100-105.

Pavelka, M. & Roth, J. (2010). Descemet's Membrane. Functional Ultrastructure: Atlas of Tissue Biology and Pathology, 2nd ed., Springer Vienna, pp. 184-185.

Perez, C.M., Panitch, A. & Chmielewski, J. (2011). A collagen peptide-based physical hydrogel for cell encapsulation. Macromolecular bioscience, Vol. 11(10), pp. 1426-1431.

Pineda, R. (2015). The KeraKlear Artificial Cornea. Cortina, M.S. & de la Cruz, J. (ed.), Keratoprostheses and Artificial Corneas: Fundamentals and Surgical Applications. Springer Berlin Heidelberg, pp. 213-219.

Price, R.D., Berry, M.G. & Navsaria, H.A. (2007). Hyaluronic acid: the scientific and clinical evidence. Journal of plastic, reconstructive & aesthetic surgery: JPRAS, Vol. 60(10), pp. 1110-1119.

Proulx, S., d'Arc Uwamaliya, J., Carrier, P., Deschambeault, A., Audet, C., Giasson, C.J., Guerin, S.L., Auger, F.A. & Germain, L. (2010). Reconstruction of a human cornea by the self-assembly approach of tissue engineering using the three native cell types. Molecular vision, Vol. 16, pp. 2192-2201.

Ruberti, J.W., Roy, A.S. & Roberts, C.J. (2011). Corneal biomechanics and biomaterials. Annual Review of Biomedical Engineering, Vol. 13, pp. 269-295.

Schrage, N., Hille, K. & Cursiefen, C. (2014). Current treatment options with artificial corneas: Boston Kpro, Osteo-odontokeratoprosthesis, Miro Cornea® and KeraKlear®. Der Ophthalmologe: Zeitschrift der Deutschen Ophthalmologischen Gesellschaft, Vol. 111(11), pp. 1010-1018.

Seidlits, S.K., Khaing, Z.Z., Petersen, R.R., Nickels, J.D., Vanscoy, J.E., Shear, J.B. & Schmidt, C.E. (2010). The effects of hyaluronic acid hydrogels with tunable mechanical properties on neural progenitor cell differentiation. Biomaterials, Vol 31(14), pp. 3930-3940.

Seiler, T., Matallana, M., Sendler, S. & Bende, T. (1992). Does Bowman's layer determine the biomechanical properties of the cornea? Refractive & corneal surgery, Vol. 8(2), pp. 139-142.

Shah, A., Brugnano, J., Sun, S., Vase, A. & Orwin, E. (2008). The development of a tissue-engineered cornea: biomaterials and culture methods. Pediatric research, Vol. 63(5), pp. 535-544.

Tan, H. & Marra, K.G. (2010). Injectable, Biodegradable Hydrogels for Tissue Engineering Applications. Materials, Vol. 3(3), pp. 1746.

Tonsomboon, K., Strange, D.G. & Oyen, M.L. (2013). Gelatin nanofiber-reinforced alginate gel scaffolds for corneal tissue engineering. Conference proceedings: Annual International Conference of the IEEE Engineering in Medicine and Biology Society, IEEE Engineering in Medicine and Biology Society Annual Conference, Vol. 2013, pp. 6671-6674.

Tseng, S.G., Prabhasawat, P., Barton, K., Gray, T., Meller, D. (1998). Amniotic membrane transplantation with or without limbal allografts for corneal surface reconstruction in patients with limbal stem cell deficiency. Archives of Ophthalmology, Vol. 116(4), pp. 431-441.

Wang, T. & Spector, M. (2009). Development of hyaluronic acid-based scaffolds for brain tissue engineering. Acta Biomaterialia, Vol. 5(7), pp. 2371-2384.

APPENDIX A: FTIR SPECTRA OF THE HYDROGEL COMPONENTS

The Appendix A consists of the FTIR curves of all the hyaluronan components used in this study. The curves of the unmodified hyaluronan, the aldehyde modified components HA-ALD1 and HA-ALD2, the hydrazide modified components HA-ADH and HA-CDH and the rat tail collagen I are presented below in Figures S1, S2, S3 and S4, in respective order.

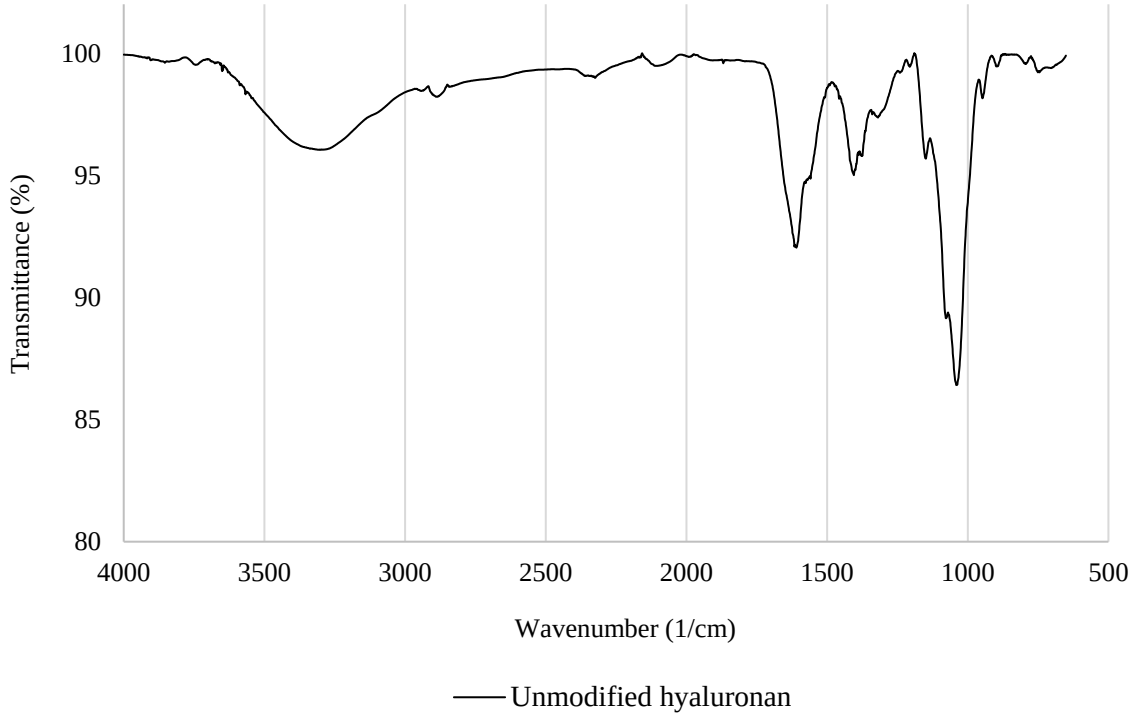

Figure S1. *The FTIR spectrum of the unmodified hyaluronan.*

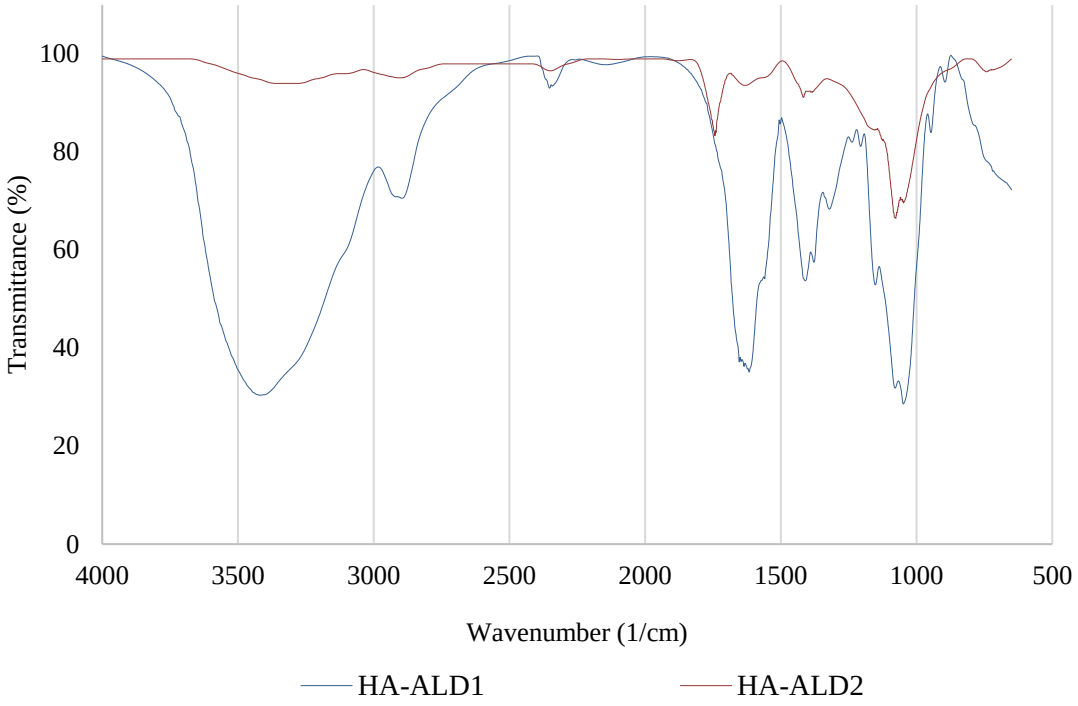

Figure S2. *The FTIR spectra of the aldehyde-modified hyaluronan components HA-ALD1 and HA-ALD2.*

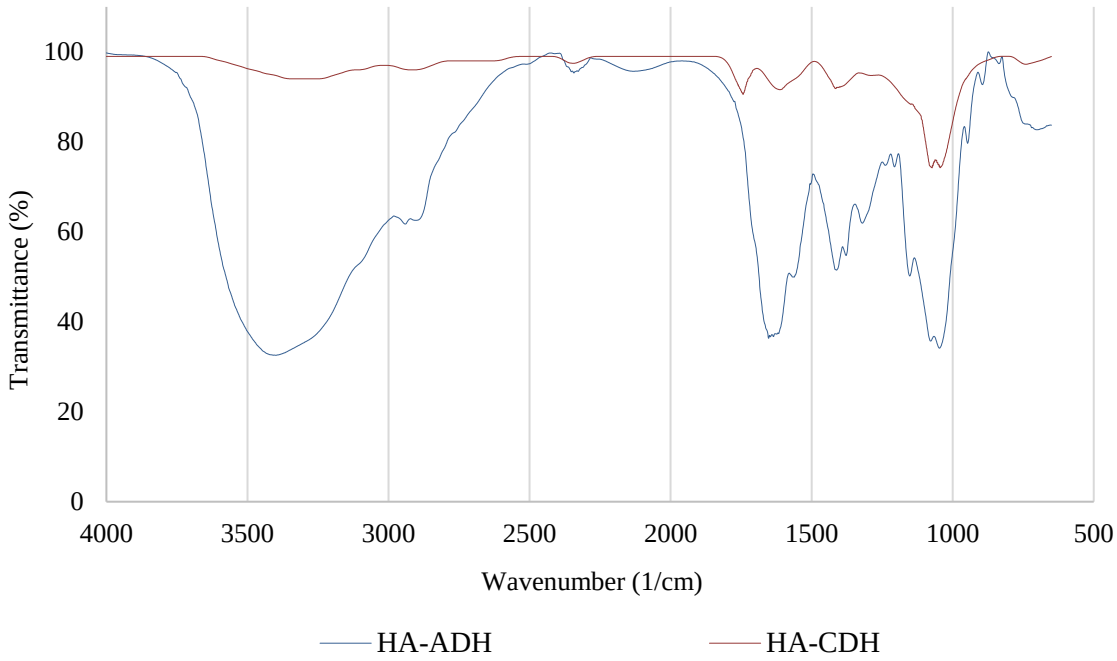

Figure S3. *The FTIR spectra of the hydrazide-modified hyaluronan components HA-ADH and HA-CDH.*

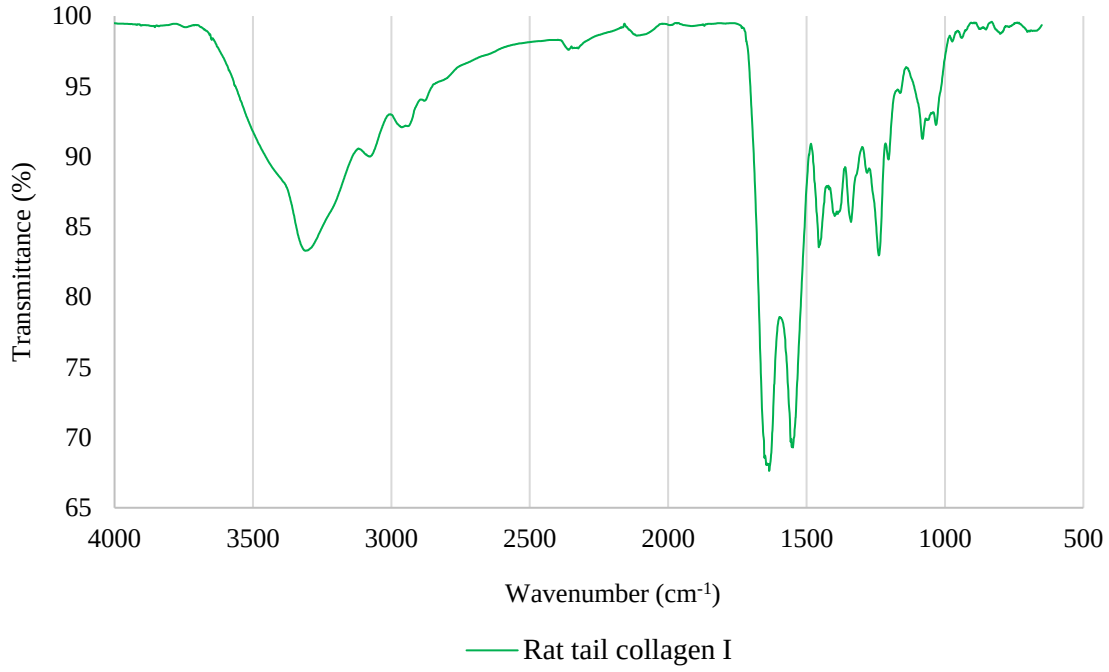

Figure S4. *FTIR spectrum of rat tail collagen I.*